Initial Characterization of the Two ClpP Paralogs of *Chlamydia trachomatis* Suggests Unique Functionality for Each

Nicholas A. Wood[1,2], Krystal Chung[3], Nathalia Rodrigues de Almeida[4], Martin Conda-Sheridan[4], Derek J. Fisher[3], Scot P. Ouellette[1#]

[1]Department of Pathology and Microbiology, College of Medicine, University of Nebraska Medical Center, Omaha, NE

[2]Division of Basic Biomedical Sciences, Sanford School of Medicine, University of South Dakota, Vermillion, SD

[3]Department of Microbiology, Southern Illinois University Carbondale, Carbondale, IL

[4]Department of Pharmaceutical Sciences, College of Pharmacy, University of Nebraska Medical Center, Omaha, NE

Keywords: *Chlamydia*, differentiation, protein turnover, protein quality control, Clp protease

Running Title: ClpP proteases of *Chlamydia*

#Corresponding Author:

Department of Pathology and Microbiology, College of Medicine, University of Nebraska Medical Center, 985900 Nebraska Medical Center (DRC2 5022), Omaha, NE

Tel: +1-402-559-0763 Fax: +1-402-559-5900 Email: scot.ouellette@unmc.edu

Abstract

Chlamydia is an obligate intracellular bacterium that differentiates between two distinct functional and morphological forms during its developmental cycle: elementary bodies (EBs) and reticulate bodies (RBs). EBs are non-dividing, small electron dense forms that infect host cells. RBs are larger, non-infectious replicative forms that develop within a membrane-bound vesicle, termed an inclusion. Given the unique properties of each developmental form of this bacterium, we hypothesized that the Clp protease system plays an integral role in proteomic turnover by degrading specific proteins from one developmental form or the other. *Chlamydia* has five uncharacterized *clp* genes: *clpX*, *clpC*, two *clpP* paralogs, and *clpB*. In other bacteria, ClpC and ClpX are chaperones that unfold and feed proteins into the ClpP protease to be degraded, and ClpB is a deaggregase. Here, we focused on characterizing the ClpP paralogs. Transcriptional analyses and immunoblotting determined these genes are expressed mid-cycle. Bioinformatic analyses of these proteins identified key residues important for activity. Over-expression of inactive *clpP* mutants in *Chlamydia* suggested independent function of each ClpP paralog. To further probe these differences, we determined interactions between the ClpP proteins using bacterial two-hybrid assays and Native gel analysis of recombinant proteins. Homotypic interactions of the ClpP proteins, but not heterotypic interactions between the ClpP paralogs, were detected. Interestingly, ClpP2, but not ClpP1, protease activity was detected *in vitro*. This activity was stimulated by antibiotics known to activate ClpP, which blocked chlamydial growth. Our data suggest the chlamydial ClpP paralogs likely serve distinct and critical roles in this important pathogen.

Words: 250/250

Importance

Chlamydia trachomatis is the leading cause of preventable infectious blindness and of bacterial sexually transmitted infections worldwide. Chlamydiae are developmentally regulated, obligate intracellular pathogens that alternate between two functional and morphologic forms with distinct repertoires of proteins. We hypothesize that protein degradation is a critical aspect to the developmental cycle. A key system involved in protein turnover in bacteria is the Clp protease system. Here, we characterized the two chlamydial ClpP paralogs by examining their expression in *Chlamydia*, their ability to oligomerize, and their proteolytic activity. This work will help understand the evolutionarily diverse Clp proteases in the context of intracellular organisms, which may aid in the study of other clinically relevant intracellular bacteria.

Words: 114/120

Introduction

Chlamydia trachomatis is one of the most prevalent human sexually transmitted infections and the leading cause of preventable infectious blindness worldwide (1). Of particular note are the negative effects associated with untreated *C. trachomatis* infections. Because of the asymptomatic nature of 60-80% of cases (2), infection by this organism can lead to complications such as pelvic inflammatory disease, which can in turn lead to infertility and ectopic pregnancies in women (3). An infant can also acquire conjunctivitis during birth should the mother be infected, which can result in irreversible blindness if left untreated.

C. trachomatis is an obligate intracellular pathogen with a complex developmental cycle (see (4) for detailed review). These pathogenic bacteria differentiate between two distinct functional and morphological forms over the course of 48 to 72 hours, depending on the strain. The electron dense elementary body (EB) is the infectious but non-dividing form that is characterized by its histone-compacted chromosome (5) and cysteine-rich, disulfide-crosslinked outer membrane (6). The reticulate body (RB) is the non-infectious and replicating form that has a relaxed chromosome structure and lipid-based cell walls that are sensitive to disruption. The typical size of each form is ~0.3 μm and ~1 μm, respectively (4). A single EB initiates infection of a host cell by attaching to the plasma membrane and inducing uptake into the cell by type III secreted effectors (7) (8). The EB remains within a host-derived vesicle, which is diverted from the endocytic pathway, and differentiates into the much larger RB. The vesicle is rapidly modified into a pathogen-specified parasitic organelle termed an inclusion (9) (10). Proliferation of this RB within the inclusion follows until such time that secondary differentiation occurs, and the RBs begin to condense their genome and crosslink their outer membrane. After a significant amount of EBs have accumulated, they exit the cell for infection of surrounding cells. Proteomic and transcriptional analyses indicate that EBs and RBs have distinct patterns of gene expression and protein repertoires (11) (12) (13) (14). Given

the striking phenotypic differences between the two developmental forms, we hypothesize that protein turnover plays a key role in differentiation in addition to general maintenance of bacterial homeostasis during both normal and persistent growth modes (15) (16) (17).

Even though *Chlamydiae* exhibit such a complex developmental cycle and evade the host immune system during chronic infections, these bacteria have undergone significant reductive evolution to eliminate unnecessary genes. This in turn suggests that most genes retained by this organism likely serve an important function to bacterial fitness (18). Within its genome, *Chlamydia* encodes homologs to four **c**aseino**l**ytic **p**rotease *clp* genes: *clpC*, *clpX*, *clpP* (*clpP1* and *clpP2*), and *clpB*. ClpB is a suspected deaggregase, but does not appear to interact directly with other Clps for proteomic turnover (12). ClpC and ClpX proteins are classified as AAA+ (**A**TPases **A**ssociated with various cellular **A**ctivities) unfoldases that serve as adaptor proteins to linearize target proteins in an ATP-dependent manner (19) (20). ATP binding, but not necessarily hydrolysis, potentiates interaction between a homo-hexamer of these proteins and a ClpP oligomer in other organisms (21) (22). ClpP is a serine protease that gives peptidase function to the resultant complex (23). ClpP proteins have been shown to oligomerize into a tetradecameric complex of a stack of two heptamers that can then perform proteolytic function of small peptide substrates. Upon interaction with the adaptor protein hexamers, the N-terminal region of the ClpP complex is relaxed and stabilized, allowing larger substrates into the proteolytic complex (24) (25).

Multiple pathogenic bacteria possess two *clpP* paralogs including *Pseudomonas aeruginosa*, *Mycobacterium tuberculosis*, and *Listeria monocytogenes*,. The Baker lab characterized the dual ClpP system of *P. aeruginosa* and demonstrated that each system may have a distinct function contributing to virulence and fitness of the bacteria (26). While the group studying ClpP1/2 in *Mycobacterium* showed heterologous interactions between these paralogs, these genes are co-transcribed, suggesting coupled function (27). The dual ClpP proteases of *Listeria monocytogenes*

(Lm) were shown to form both hetero- and homotypic complexes (28) (29), yet the authors demonstrated that Lm ClpP2 likely can function independently of Lm ClpP1. These studies, taken together with the reductive evolution of the chlamydial genome, led us to hypothesize that the chlamydial ClpPs may serve distinct and critical functions in the physiology of the organism.

To begin investigation of the role of the Clp protease system in chlamydial biology, we initiated a series of studies to characterize the ClpP paralogs. All *clp* genes are transcribed as RB-specific genes, and the translated product of *clpP2* was detected during the developmental cycle. Bioinformatic and structural modeling analyses indicate that these proteins retain key residues important for function as well as structure. Interestingly, over-expression of a mutant ClpP1 was detrimental to chlamydial development whereas a mutant ClpP2 had no observable effect. To explore the basis of this observation, we performed a series of *in vitro* and *in vivo* assays indicating homo-oligomerization of each paralog. However, we did not detect hetero-oligomerization between these paralogs. We also characterized the *in vitro* protease activity of each ClpP paralog and observed that activity was only detected for ClpP2. Antibiotics known to activate ClpP proteases stimulated the protease activity of ClpP2 only and blocked chlamydial growth. Combined, our data suggest ClpP1 activity may be tightly regulated. We conclude that each chlamydial ClpP protease serves a unique and independent role, either in differentiation or more typical physiological processes.

Results

The *clp* genes are expressed as RB specific genes. We hypothesize, based on the arrangement of the genes in the chromosome, that ClpC interacts with ClpP1 and that ClpX interacts with ClpP2. This does not preclude each individual component from acting independently and is not mutually exclusive to our hypothesis. We base our prediction of ClpP2X interaction due to the juxtaposition of

the two genes within the same operon (Fig. 1A). We then reasoned that ClpP1 would serve as the proteolytic subunit that would interact with ClpC, as both are encoded independently of each other in separate genomic contexts (Fig. 1A). Because chlamydiae are developmentally regulated bacteria, gene expression can differ from one developmental form to the other. Gene expression in *Chlamydia* can be broadly categorized into three different stages: early-, mid-, and late-developmental cycle genes (30). Early cycle genes are involved in initial differentiation from EB to RB and establishment of the nascent inclusion. Mid-cycle genes are RB specific and typically play a role in growth and division of the RBs as well as in inclusion modification. Late cycle genes function in differentiation from an RB to an EB or serve an important function in the secondary infection of a host cell. The specificity of a transcript to a particular point of the developmental cycle can give insight into the possible function of the encoded protein. To determine when during the developmental cycle the *clp* genes are transcribed, we measured the transcription of each gene over a time course of infection. Nucleic acid samples were collected for analysis at various time points of infection using wild-type *C. trachomatis* serovar L2. Our data indicate that the *clp* genes analyzed are transcribed in a pattern consistent with mid-cycle, RB specific function since the transcript levels peak after primary differentiation has occurred and a population of RBs has been established (i.e. 16 hpi; Fig. 1B). This pattern is distinct to that of canonical early or late cycle genes such as *euo* or *omcB* (31) (32) (33). The *clpX* transcript levels closely mirrored those of *clpP2* albeit with slightly lower transcript abundance, consistent with its genomic context 3' to *clpP2*.

We next sought to detect endogenous protein of the ClpP paralogs. Given the high level of homology between the *Pseudomonas aeruginosa* (Pa) ClpP1 and *C. trachomatis* (Ctr) ClpP2 (see Fig. 2), we speculated a polyclonal antibody developed against Pa_ClpP1 (kind gift of Dr. T. Baker, MIT) would detect Ctr ClpP2 by Western blot (see Suppl. Fig. S1). As seen, Ctr ClpP2 was detected from infected cell lysates starting at 16h post-infection using the polyclonal anti-Pa_ClpP1 antibody

(Fig. 1C). The polyclonal antibody developed against Pa_ClpP2 did not react with chlamydial lysates or recombinant Ctr ClpP1 or ClpP2 (Suppl. Fig. S1). Given the relatively low levels of ClpP2 compared to the major outer membrane protein (MOMP; Fig. 1D), we cannot conclude that ClpP2 is not present at earlier times or that an antibody specific to chlamydial ClpP2 would be more sensitive to detect such lower levels. We are currently working towards developing antibodies against the chlamydial Clp components. Overall, the expression data indicate that the Clp components are expressed in the RB phase of growth and division. This does not, however, preclude these proteins from having functions at other times during the developmental cycle.

Bioinformatics analyses identify key residues important for structure and function of each chlamydial ClpP paralog. We hypothesized that each ClpP paralog of *C. trachomatis* serves distinct functions in the biology and pathogenesis of this unique bacterium, despite their similarity in expression patterns. To further test this hypothesis, we performed a series of bioinformatics analyses. We began by looking at pairwise alignments of the chlamydial ClpP proteins against each other and against ClpP homologs from other bacteria (Fig. 2A). Interestingly, each chlamydial ClpP shared more homology to ClpP of *E. coli*, at 44% and 55% identity with Expect values of $4x10^{-51}$ and $2x10^{-83}$, respectively, and to other ClpP homologs than to its paralog. This observation was supported by the ability of the anti-Pa_ClpP1 antibody to recognize Ctr ClpP2 (Fig. 1C). The sequence identity between Ctr ClpP1 and Ctr ClpP2 is 39% with an Expect value of 10^{-44}. Similarly, the two ClpP paralogs of *P. aeruginosa* also share a low amount of similarity to each other compared to other ClpP homologs via protein alignment (data not shown), and each serves a distinct function in *P. aeruginosa* (26). Therefore, these observations support the likelihood that the chlamydial ClpP paralogs have distinct roles.

A closer analysis of the chlamydial ClpP paralogs provides further evidence for unique functionality of each protein. A 3-dimensional predicted structure alignment of Ctr ClpP1 and ClpP2 to *E. coli* ClpP indicates that the structural architecture would allow for homo-oligomer formation and interaction with chaperones (Fig. 2B), though distinct differences in the oligomer interface may prevent hetero-oligomerization (34). Additionally, the catalytic triad active site aligns well for all ClpP homologs analyzed (Fig. 2B&C), with variation in structure being mostly limited to the N- and C-termini. Also unique to chlamydial ClpP1 are distinct differences at residues that align to amino acids critical to activation in other bacteria. An alanine at position 37 of Ctr ClpP1 may result in a conformational difference in the P1 pre-activation complex that precludes P1/P2 interaction (35). This may serve a regulatory role. Further supporting differential regulation is the lack of an aromatic amino acid at position 57 of ClpP1 that is relatively well-conserved in other ClpP homologs, suggesting that Ctr ClpP1 enters the "open" conformation differently than Ctr ClpP2. Ongoing studies are investigating these residues in addition to others that are involved in complex activation. Given the conserved catalytic residues and the structural similarity of the Ctr ClpP proteins to homologs from a diverse set of bacteria, we conclude that the chlamydial ClpP proteins are *bona fide* protease subunits. However, the predicted structural differences at the termini of the protein and in other key residues suggests that the chlamydial ClpP proteins (i) do not interact with each other, (ii) have specialized functions, and (iii) are regulated differently.

Overexpression of inactive ClpP1, but not ClpP2, negatively affects *Chlamydia*. Leveraging recent advances in chlamydial genetics, we next determined the effect of over-expression of ClpP proteins in *Chlamydia*. We designed and constructed plasmids encoding wild-type or inactive mutants of each *clpP* paralog, fused to a 6xHis tag, under the control of an anhydrotetracycline (aTc)-inducible promoter (36). Interestingly, we were unable to successfully transform *C.*

trachomatis serovar L2 with plasmids encoding the wild-type *clpP* genes. The reasons for this are unclear (aside from the inherent difficulty in transforming this obligate intracellular bacterium) but may indicate that leaky expression from the promoter was deleterious to the organism (37). However, we successfully transformed *C. trachomatis* with plasmids encoding either ClpP1 S92A or ClpP2 S98A active site serine mutants that are known to abolish protease activity (See Fig. 2B; (38)). To assess the effect of over-expression of these inactive mutants, HEp2 cells were infected with each transformant and expression was induced at 10 hours post-infection with 1 or 10 nM aTc. Both 6- and 14-hour pulses were utilized to determine inclusion morphology at 16 and 24 hours post-infection, respectively. At each time point and at the lower concentration of aTc inducer, the localization of the ClpP proteins was within the bacterial cytosol. No noticeable effects were detected after 6h of induction for the ClpP2 mutant, while the ClpP1 mutant induction appeared to have a slight negative impact on the organisms. However, after 14h of over-expression of the mutant ClpP1, noticeably smaller inclusion sizes were observed (Fig. 3A) whereas over-expression of the mutant ClpP2 had no demonstrable effect (Fig. 3B). These data indicate that over-expression of ClpP1 S92A is detrimental to chlamydiae. In support of this conclusion, we were unable to isolate a clonal population of purified ClpP1 S92A transformants as we routinely observed bacterial populations susceptible to antibiotic selection even after multiple passages. This observation indicates that leaky expression may drive plasmid loss as has been observed in other chlamydial transformation systems (37, 39).

The ClpP paralogs demonstrate homotypic, but not heterotypic, interactions. To better understand the function of each ClpP paralog and why over-expression of ClpP1 S92A, but not ClpP2 S98A, was detrimental to *Chlamydia*, we initiated a series of *in vivo* and *in vitro* biochemical assays to characterize the properties of the ClpP proteins. Extensive evidence exists from other

bacterial systems to indicate that ClpP forms a tetradecameric complex composed of two heptameric rings (21-25, 40, 41). To determine whether the chlamydial ClpP paralogs formed homo- and/or heterooligomers, we first employed the bacterial adenylate cyclase-based two-hybrid (BACTH) system to detect protein-protein interactions. This *in vivo* assay is based on the reconstitution of adenylate cyclase activity when two functional fragments of Cya from *B. pertussis* are brought into close proximity by interacting proteins (42). Interactions can be qualitatively determined on Xgal plates and quantified by beta-galactosidase activity. Using the BACTH system, we observed homo-oligomerization of each ClpP paralog, but failed to detect interactions between ClpP1 and ClpP2 (Fig. 4A&B). Importantly, the active site mutants also interacted with each other, indicating that this mutation did not interfere with homo-oligomerization. These data are consistent with the predicted structural and sequence differences noted (Fig. 2B&C).

As the BACTH system cannot indicate oligomerization state, we next purified recombinant chlamydial ClpP1 and ClpP2 (22 and 23 kDa, respectively), including the active site mutants, and analyzed their migration by native PAGE. As a positive control, we also purified *E. coli* ClpP (24 kDa). Each of the recombinant chlamydial proteins clearly formed a heptamer with a fainter, slower migrating band indicating potential tetradecamer forms (Fig. 4C). The *E. coli* ClpP, in contrast, migrated primarily as a tetradecamer with a less intense band at the predicted size of a heptamer. In purifying Ctr ClpP1, we noticed the presence of a doublet band (Suppl. Fig. S2). However, the N-terminus encodes two additional methionine residues at positions 6 and 7, thus the smaller product may have resulted from an alternative start site when expressed in *E. coli*. Mass spectrometry analysis of the N-terminus of each band supported this conclusion (Suppl. Fig. S2). To ensure that only the larger, full-length product was produced, we mutated the methionine residues to leucine and isoleucine. This recombinant ClpP1 (M6L/M7I) also migrated predominantly as a heptamer in the

Native PAGE assay (Fig. 4C). Therefore, we conclude that the smaller product did not alter the oligomerization state of the protein.

Both our bioinformatics predictions and the BACTH data indicated that ClpP1 and ClpP2 do not interact. To further test this, we mixed each recombinant protein in equimolar amounts and analyzed their oligomerization state by Native PAGE. In support of our early observations, we did not observe heteromers of each ClpP paralog as each protein ran as distinct heptamers with no intermediate bands indicative of mixing of the monomers (Fig. 4D). However, we can neither exclude that the *in vitro* conditions preclude an interaction between these components nor that these paralogs interact *in vivo*. Nevertheless, given the differences in predicted structures at the termini of each ClpP paralog (Fig. 2) and the different interaction data presented here, the parsimonious interpretation is a model wherein each protease complex functions separately.

Chlamydial ClpP1 and ClpP2 vary in protease activity *in vitro*. To determine the functionality of the protease complexes, we used the recombinant chlamydial ClpP proteins to assess their ability to degrade the small, fluorogenic compound Suc-LY-AMC. The degradation of this compound by other bacterial ClpP enzymes does not rely on ClpP activation by AAA+ chaperone complexes (43), thus we could probe the basal protease activity of the ClpP paralogs. While ClpP2 degraded the substrate under our given assay conditions, ClpP1 activity could not be detected (Fig. 5A). This result for ClpP1 was not due to the presence of the alternative start site product since the M6L/M7I mutant displayed no activity in this assay. We also observed enhanced protease activity for ClpP2 in a sodium citrate buffer, as noted by others (44), but this buffer did not stimulate ClpP1 activity. That ClpP1 lacks the ability to degrade Suc-LY-AMC suggests the N-terminal region of the complex (Fig. 2) may block entry of even this small reporter substrate into the active site. Importantly, the activity of the ClpP2 protease was abolished by the active site serine mutation S98A (Fig. 5B). As a positive

control, we also tested the activity of the *E. coli* ClpP complex in our assay conditions and observed degradation of the Suc-LY-AMP compound that was increased by sodium citrate (Fig. 5C). Thus, in spite of the activity of chlamydial ClpP2, it displayed a significantly lower proteolytic capacity *in vitro* compared to the *E. coli* ClpP. The apparent preference of heptameric formation by both chlamydial ClpP1 and ClpP2 could explain the reduced activity as compared to the *E. coli* ClpP, which preferentially formed tetradecamers *in vitro* (see Fig. 4C). These observed differences suggest either that the assay conditions, which work for other bacterial ClpP homologs, are not optimal for chlamydial ClpP proteases or that *Chlamydiae* tightly regulate the activity of their ClpP complexes.

ClpP-activating antibiotics stimulate protease activity of ClpP2, but not ClpP1, and block chlamydial growth. Recently, a novel class of antibiotics that target ClpP have been developed (45). ACP and ADEP derivatives activate ClpP by eliminating or reducing its need for chaperone binding. The unregulated proteolysis that results has been demonstrated to eliminate persister bacteria (46). We used these compounds to determine whether the activated chlamydial ClpP proteases could degrade a more complex substrate, casein. As noted with the Suc-LY-AMP substrate, ClpP1 failed to degrade casein in the presence of any of the ACP1 derivatives (Fig. 6A). By contrast, the ACP1 compounds stimulated ClpP2 to degrade casein (Fig. 6B), albeit with some detectable substrate remaining at the end of the assay. As before, the *E. coli* ClpP was more efficient in degrading the substrate with little to no casein detectable at the end of the assay (Fig. 6C; (47)). ClpP2 was thus able, in the presence of these drugs that relax the N-termini of the complex, to degrade larger substrates with intrinsically disordered regions (i.e. casein). The inability to detect proteolytic activity of ClpP1 again suggests that additional factors may regulate its activity consistent with the differences we observed in our bioinformatics analysis (Fig. 2). Also consistent with the difference in activation is the lack of an aromatic amino acid at residue 57 of ClpP1. This particular residue of

the hydrophobic pocket has recently been shown to be instrumental in ADEP-induced dysregulation of proteolytic activity, which supports a model where chlamydial ClpP1 is unaffected by activating drugs (35). However, we cannot exclude that we have not identified the optimal conditions necessary to demonstrate the enzyme activity of wild-type ClpP1.

As we were able to demonstrate the ability of the ACP1 compounds to activate ClpP2, we next sought to test the effect of these compounds directly on *Chlamydia* growth and viability. To ensure that any effect on the bacteria was not due to host cell death, we first tested cell viability of infected, ACP-treated HEp2 cells. Indeed, we noted limited loss (~10%) in host cell viability for both 25 and 50 μg/mL concentrations following 16 hours of drug treatment (Fig. 6D), which reinforces that any loss of bacterial viability would not be due to a reduction in host cell viability. The ACP drugs all showed a remarkable impact on *Chlamydia* at both concentrations tested (Fig. 6E). The lower drug concentration resulted in a 50-fold reduction in recoverable EBs when added at 8 hours post-infection whereas the higher concentration led to almost complete abrogation of chlamydial viability. Given the effects of the ACP compounds on ClpP protease activity *in vitro*, these data suggest that uncoupling of ClpP2 activity from its cognate ATPase strongly inhibits chlamydial growth.

Discussion

The Clp protease system has been extensively characterized in *E. coli* and *Bacillus subtilis*, and its importance in the growth and virulence of various pathogens (opportunistic or not) has been examined (see (23) for review). Since the discovery of the ClpP protease (48), interaction studies demonstrated that the ClpP proteins typically interact as a tetradecameric stack of two heptamers (49). The serine active sites are buried within these barrel-like structures (50). ClpP hydrolysis of large protein substrates is increasingly stimulated in the presence of AAA+ chaperone binding (51).

However, complexed ClpP alone processes small substrates of up to 30 amino acids regardless of the presence of ATP, suggesting that active site availability and complex accessibility are the two main mechanisms regulating ClpP activity (52). Substrates that enter this complex by either chaperone-mediated or chaperone-independent means are hydrolyzed into short peptides of 6-8 amino acids with some degree of amino acid specificity (44, 53).

While not unprecedented, the presence of two encoded *clpP* paralogs in a bacterial chromosome is unusual. In *P. aeruginosa*, another bacterium encoding dual ClpP proteases, the two isoforms have not been shown to interact in any test condition, and the different transcriptional profiles and differential effects on virulence factor production indicate these paralogs likely have distinct roles in *P. aeruginosa* (26). Conversely, the two ClpP proteins of *M. tuberculosis* and *L. monocytogenes* heterologously interact as two homotypic heptamers, which facilitates an increase in function (27, 29, 54). The activation of one homotypic ClpP heptamer activates the heptamer of the other isoform in *M. tuberculosis*, providing a novel mechanism for activation (41). Of note is that *L. monocytogenes* ClpP2 may also form a completely homotypic tetradecamer of one ClpP paralog (55). Again, the Clp proteolytic subunits play an integral role in virulence factor regulation in addition to enhancement of bacterial survival during intracellular growth (56). Taken together, these studies demonstrate the diverse function of dual ClpP peptidase systems in the pathogenesis and growth of various bacteria.

The work presented here to characterize the *C. trachomatis* ClpP paralogs is the first to explore the function and role of the Clp protease system in chlamydiae. Our results suggest that the two ClpP proteases likely serve distinct roles in chlamydial physiology and, we hypothesize, in the complex developmental cycle of this organism. We utilized bioinformatics techniques as an initial approach to investigate the potential function of the ClpP proteins. We observed significant similarity of the chlamydial ClpP paralogs to ClpP homologs of more studied organisms such as *E.*

coli. In support of this, most of the hallmark conserved residues, including the active site triad, are present in the chlamydial ClpP paralogs. Both ClpP1 and ClpP2 have hydrophobic residues aligned with those of other bacterial ClpPs, suggesting the presence of AAA+ adaptor protein docking sites (57). Indeed, chlamydial ClpC and ClpX encode the evolutionarily retained IGF/L loop motifs that facilitate interaction with the ClpP tetradecameric complex (Wood and Ouellette, unpublished observation) (41). In spite of the similarities between the ClpP paralogs, there are also notable differences. The C-termini of both chlamydial ClpPs contain two residues that comprise the hydrophobic pocket (47, 58), but the alignment shows the presence of charged residues (D15, K40, K41, and D66) in ClpP1 while the conserved residues appear to be uncharged. In addition, ClpP1 lacks a highly conserved tyrosine residue (D15), a conserved glutamine (A36), and a conserved aromatic residue (V57), all of which contribute to canonical activation and tetradecamer chamber access for other homologs (35). Of note is the predicted alpha helix at the N-terminus of ClpP1 and the C-terminus of ClpP2, which may contribute to some form of steric hindrance to prevent interaction between ClpP1 and ClpP2 (59). Indeed, we could not detect an interaction between ClpP1 and ClpP2 using both *in vivo* and *in vitro* techniques. Rather, we detected only homoheptameric oligomers. While our *in vitro* assays have failed to show P1/P2 complex formation, we cannot rule out the possibility of protein modification *in vivo* promoting heteromers. Further studies examining the role of the N- and C-termini will be conducted to determine whether or not they play a role in complex formation and/or specificity.

Given the role of the N-terminal regions in regulation of the ClpP protease via reduced access into the proteolytic complex (60), the hypothesis of a difference in interaction or regulation of the ClpP complexes in *C. trachomatis* is reasonable based on the data presented here. We detected ClpP2 protease activity against both a small oligopeptide substrate and the more complex casein substrate. However, we did not detect proteolytic activity of ClpP1 *in vitro*, even in the presence of

368 well-characterized drugs that activate ClpP complexes in the absence of an ATPase, which is in
369 agreement with an important and highly regulated role for ClpP1 in *C. trachomatis*. The structural
370 conservation and presence of the catalytic active site makes it unlikely that ClpP1 is a catalytically
371 inactive protease. Rather, some form of modification or conformational change in structure, possibly
372 chaperone or adaptor mediated, may be necessary to promote full complex formation and activity
373 both *in vitro* and *in vivo*. In this model, an unknown regulatory factor may modulate ClpP1 activity.
374 In a manner consistent with our bioinformatics data, ClpP1 may be activated non-canonically, as the
375 mechanism needed to open the channel at the V57 residue is likely different than those targeting the
376 aromatic amino acids present in other homologs. We are investigating this and other possibilities.

377 Our data lead us to hypothesize that each ClpP protein in *Chlamydia* forms a separate
378 protease complex and, therefore, serves a different function. Whether each ClpP interacts
379 specifically with ClpX or ClpC remains to be determined. However, the genomic proximity of ClpP2
380 to ClpX suggests a likely interaction with ClpX by sequestration immediately following translation;
381 thus, we speculate that ClpP1 likely interacts preferentially with ClpC. Our qPCR data suggest that
382 the *clpX*-encoding gene follows the *clpP2*-encoding gene in an operon, further supporting coupled
383 function and an *in vivo* complex of ClpP2 and ClpX oligomers. Complex formation is currently
384 under investigation as is what role each complex has *in vivo*. It is also possible that ClpP
385 tetradecamers may function independently *in vivo* in a housekeeping role to degrade small
386 oligopeptides resulting from degradation of larger proteins and/or import from the host cell.
387 *Chlamydiae* encode a large repertoire of oligopeptide transporters, and the short peptide substrates
388 are an important source of nutrients, particularly early during infection (61).

389 One of the unexpected outcomes of these initial studies was the failure to transform *C.*
390 *trachomatis* with wild-type ClpP constructs. Tet-inducible systems have reduced leakiness compared
391 to other inducible expression systems (62) (63), and this leakiness has been observed in constructs

used to transform *C. trachomatis* (37). When used for the expression of essential gene products or in situations where gene dosage effects are important, the leaky expression can lead to plasmid loss and/or the inability to transform *Chlamydia*. Based on repeated failure to transform *C. trachomatis* with vectors encoding the wild-type ClpP proteins, we conclude that leaky expression led to rejection of the plasmid (see also (37)). This suggests that stoichiometric ratios of functional Clp enzymes are important to bacterial homeostasis. In spite of the failure to transform *C. trachomatis* with wild-type ClpP expressing vectors, we were successful in transforming *C. trachomatis* with vectors encoding catalytically inactive ClpP mutants. Interestingly, over-expression of the inactive ClpP mutants in *Chlamydia* resulted in differential effects on chlamydial growth and morphology. ClpP2 S98A has, even upon the highest level of induction, little negative effect on inclusion morphology. The disconnect between the transformation of wild-type and inactive mutants could mean that the ratio of wild-type ClpP2 to its cognate AAA+ chaperone is vital, perhaps to prevent unregulated proteolysis, but incorporation of inactive forms of ClpP2 (activity loss confirmed *in vitro*, see Fig. 5B) into the tetradecameric oligomer is not necessarily harmful to *C. trachomatis*. The ability of ClpP2 to degrade a small peptide reporter (Fig. 5A) is in congruence with a model where a chaperone-independent ClpP2 tetradecamer targets and degrades imported peptides. Given that overexpression of inactive ClpP2 seems to have limited negative impact on chlamydial development, an inactive ClpP2 oligomer may bind small peptides, preventing extensive targeting of other, more vital substrates and negating any dominant negative effect. Conversely, over-expression of ClpP1 S92A and its incorporation into the endogenous ClpP1 proteolytic machinery has a clear negative impact on *Chlamydia*. We observed that the mutant ClpP proteins interacted with the wild-type proteins in the BACTH assay (Wood and Ouellette, data not shown), suggesting the potential of the inactive proteins to form complexes with the endogenous proteins. Overall, these data suggest that, should each mutant protein oligomerize with endogenous wild-type protein *in vivo*, subunit

poisoning of the ClpP1 complex is deleterious to chlamydiae whereas the ClpP2 complex is more tolerant.

We hypothesize that proteolytic Clp subunit regulation by a chaperone protein is vital to chlamydial survival. Based on our studies with the ACP1 antibiotics, our assays showed that ClpP2 acts in a manner similar to other well-characterized ClpP proteases when artificially activated by these compounds (Fig. 6A&C). Consequently, treatment of *Chlamydia*-infected cells with ACP1 (or one of its derivatives) significantly and drastically reduced chlamydial growth (Fig. 6E), which we speculate is due to the effects on ClpP2 function. Whether the negative effect stems from dysregulation of ClpP2 leading to uncontrolled proteolysis, which is supported by the *in vitro* degradation of casein, or from blocking of ClpP2/AAA+ chaperone complex formation, resulting in the inability to degrade larger substrates not accessible to ClpP2 alone, is currently under investigation. In spite of the inability of ClpP2 S98A over-expression to significantly impact chlamydial growth, the antibiotics data suggest that disruption of ClpP2 via dysregulation of activity is overwhelmingly negative to chlamydial physiology. However, we cannot exclude a possible effect of these antibiotics on ClpP1 *in vivo*. Clearly, over-expression of ClpP1 S92A was deleterious to chlamydial growth, thus we conclude that each ClpP paralog is essential to normal growth and development.

We have shown here an initial characterization of the chlamydial Clp protease system focusing on the ClpP protease components. Overall, the sensitivity of the organisms to perturbations in ClpP activity suggests a critical function for these paralogs in maintenance of chlamydial physiology. We speculate that these systems will also play an integral role in differentiation and possibly persistence (64) (65), which may provide a mechanism that could be leveraged to block growth or eliminate persister cells (46). Further characterization of the chlamydial Clp system could facilitate development of targeted therapeutics for treatment of *C. trachomatis* infection, thereby

lowering dependence on broad-spectrum antibiotics. Ongoing efforts are investigating this hypothesis as well as the function of the AAA+ chaperones.

Materials and Methods

Strains and Cell Culture: The human epithelial cell line HEp2 was utilized in the transcriptional and antibiotic studies and was routinely cultivated and passaged in Iscove's Modified Dulbecco's Medium (IMDM, Gibco/ThermoFisher; Waltham, MA), and 10% FBS (Sigma; St. Louis, MO). McCoy mouse fibroblasts were used for the purpose of chlamydial transformation, and human epithelial HeLa cells were used for plaque purification of the resulting chlamydial transformants as well as for protein isolation and assessment of ClpP2 expression. All of these cell lines were passaged routinely in Dulbecco's Modified Eagle's Medium (DMEM, Gibco/ThermoFisher). Density gradient purified *Chlamydia trachomatis* L2/434/Bu (ATCC VR902B) EBs were used for the antibiotic studies. *C. trachomatis* serovar L2 EBs (25667R) naturally lacking the endogenous plasmid were prepared and used for transformation [see (66)].

Transcript Analysis Using RT-qPCR:

HEp2 cells seeded in 6-well plates were infected at a multiplicity of infection of 1 with *C. trachomatis* serovar L2. At the indicated times post-infection, total RNA and DNA were collected from duplicate wells (65). Briefly, total RNA was collected from infected cells using Trizol reagent, extracted with chloroform, and the aqueous phase precipitated with an equal volume of isopropanol according to the manufacturer's instructions (ThermoFisher). DNA was removed from total RNA by rigorous DNase-free treatment (ThermoFisher) before 1 µg was reverse transcribed with Superscript III RT (ThermoFisher). Equal volumes of cDNA were used for qPCR. Total DNA was collected from infected cells by trypsinizing the cells, pelleting for 5 min at 400 xg, and resuspending in PBS.

Samples were freeze-thawed three times before processing with the DNeasy Blood and Tissue kit according to the manufacturer's instructions (Qiagen). 150 ng of total DNA were used for qPCR. Transcripts and genomic DNA were quantified by qPCR in 25 µL reactions using 2x SYBR Green Master Mix in an ABI7300 thermal cycler in comparison to a standard curve generated from purified *C. trachomatis* L2 genomic DNA. Transcripts were normalized to genomic DNA.

C. trachomatis *propagation and detection of ClpP2:* DFCT28, a GFP-expressing *C. trachomatis* 434/Bu clone (67), was routinely grown in and titered (using the IFU assay) on HeLa cells (68). Briefly, cells were maintained in Dulbecco's modified Eagle medium (DMEM) supplemented with 10% fetal bovine serum (FBS) and grown at 37 °C with 5% CO_2. For chlamydial infection experiments, HeLa cells were grown until confluent in 6-well tissue culture dishes and then infected with DFCT28 at an MOI of ~3 using centrifugation at 545 xg for one hour. The infected cells were then incubated at 37 °C with 5% CO_2 with DMEM/FBS supplemented with 0.2 µg/mL cycloheximide and 1x non-essential amino acids. At various times post infection, the medium was removed, cells were washed twice with 2 ml of PBS, and cells were lysed via addition of 200 µL Laemmli buffer with β-mercaptoethanol followed by heating at 90-100 °C for 5 minutes. Chlamydial protein samples or purified, recombinant ClpP samples were run on 12% SDS-PAGE gels and either stained for total protein with Coomassie Brilliant Blue or transferred to nitrocellulose for western blotting. Blots were probed with a rabbit polyclonal anti-Pa_ClpP1 (*Pseudomonas aeruginosa* designation, similar to ClpP2 from *C. trachomatis*) diluted 1:10000 in 5% milk Tris-buffered saline (mTBS) or anti-Pa_Clp2 (*Pseudomonas aeruginosa* designation, similar to ClpP1 from *C. trachomatis*) at 1:2500. The antibodies were kindly provided by Dr. T. Baker (Massachusetts Institute of Technology) (26). After incubating with primary antibodies, blots were washed with Tween (0.5%)-TBS (TTBS) and then probed with a goat, anti-rabbit IgG poly-HRP conjugated

secondary antibody (Thermo Scientific 32260) diluted 1:1000 in mTBS. As a control for chlamydial protein, blots were also probed for the major outer membrane protein (MOMP) using a mouse monoclonal anti-MOMP antibody (1:1000; Abcam, ab41193) and a goat anti-mouse IgG HRP conjugated secondary antibody (1:2000; Millipore AP124P). After incubation with the secondary antibodies, blots were washed with TTBS followed by TBS and then incubated with chemiluminescent substrate (EMD Millipore Immobilon ECL) for imaging on a Bio-Rad Chemidoc MP.

Bioinformatics Analysis: Gene maps and sequences of genes of *Chlamydia trachomatis* used were obtained from STDGen database (http://stdgen.northwestern.edu). RefSeq protein sequences from *E. coli*, *B. subtilis*, *M. tuberculosis*, and *P. aeruginosa* were acquired from the NCBI protein database (https://www.ncbi.nlm.nih.gov/guide/proteins/). The ClpP1 vs. ClpP2 protein alignment to find sequence identity was performed using NCBI Protein BLAST function (https://blast.ncbi.nlm.nih.gov/Blast.cgi) (69). Multiple sequence alignments were performed using Clustal Omega (70) with default settings and were presented using Jalview Version 2 (71). PDB files for predicted 3D structures were acquired from the Phyre2 website (http://www.sbg.bio.ic.ac.uk/phyre2/html/page.cgi?id=index) (72). Protein models and model alignments were rendered using the UCSF Chimera package from the Computer Graphics Laboratory, University of California, San Francisco (supported by NIH P41 RR-01081) (73).

Plasmid Construction: A full list of the primers and plasmids used is included in the supplementary material (S1). Plasmids for the Bacterial Adenylate Cyclase Two-Hybrid (BACTH) system were cloned using the Gateway® recombination system (74). The genes were amplified from *Chlamydia trachomatis* L2 genomic DNA with primers designed to add an *attB* recombination site on either side

of the gene. The PCR products were then incubated with a pDONR™221 entry vector (containing *attP* recombination sites) in the presence of BP Clonase II (Invitrogen) that inserts the gene via the flanking *attB* sites and removes *ccdB* endotoxin flanked by the *attP* sites encoded on the plasmid, allowing for positive selection. The result of the BP reaction was an entry vector containing the gene of interest flanked by *attL* sites. 2 µL were transformed into DH5α chemically competent *E. coli* and plated onto an LB agar plate containing 50 µg/mL kanamycin. Plasmid from an individual colony was purified and used for the LR reaction into one of three destination vectors (pST25-DEST, pSNT25-DEST, or pUT18C-DEST). The same entry vector for any given gene was used for all three LR reactions to insert into the destination vector with LR Clonase II. 150 ng of the entry vector was incubated with 150ng of destination vector for 1 hour at room temperature. 2 µL were used to transform XL1 *E. coli*, which were plated on the appropriate selection plate. Purified plasmid from an individual colony was sequence verified prior to use the in BACTH assay (see below).

Constructs for chlamydial transformation were created using the HiFi Cloning (New England Biolabs) protocol. To add the C-terminal 6xHis tag to the Clp proteins, the genes were amplified from the genome with a primer to add the poly-histidine tag. These products served as the template for PCR reactions to add the necessary overlap for the HiFi reaction. Primers were generated using the NEBuilder® assembly tool available from New England BioLabs (http://nebuilder.neb.com). The backbone used was the pTLR2 derivative of the pASK plasmid (36). The pTLR2 backbone was digested using FastDigest BshTI and Eco52I restriction enzymes and dephosphorylated using FastAP (ThermoFisher), and then 50ng of digested plasmid was incubated with a 2:1 ratio of insert copy number to backbone and 2x HiFi master mix (NEB). Following a 15 minute incubation of the reaction mix at 50° C, 2 µL of the reaction was transformed into DH5α chemically competent *E. coli* (NEB) and plated on the appropriate antibiotic selection plate. Positive clone sequences were verified by Eurofins Genomics. Sequence verified plasmids were transformed into *dam-/dcm- E. coli*

(New England BioLabs) in order to produce demethylated plasmid, which was sequence and digest verified prior to transformation into *C. trachomatis* (see below).

Strains created or used in this study are listed in the supplementary material. *E. coli* strains were maintained on LB agar plates and grown in LB medium or on LB agar plates supplemented with 100 µg/ml ampicillin as needed. Chlamydial genomic DNA for cloning was obtained from EBs using a phenol:chloroform extraction after extensive heat treatment in the presence of proteinase K (75), and *E. coli* genomic DNA was isolated using sodium hydroxide lysis of colonies. The chlamydial *clpP1* and *clpP2* along with *clpP* from *E. coli* were amplified via PCR using the primers listed in Supplemental Information and Phusion DNA polymerase (Thermo Scientific). PCR products were cloned into the pLATE31 expression vector from Thermo Scientific as directed by the manufacturer to create fusion proteins with a C-terminal 6x His-tag. Plasmids were initially transformed into *E. coli* NEB10 and selected on LB agar ampicillin plates. Transformants were screened for inserts using colony PCR with Fermentas Master Mix (Thermo Scientific) and positive clones were grown for plasmid isolation (GeneJet Plasmid Miniprep Kit, Thermo Scientific). DNA inserts were sequenced by Macrogen USA and sequence-verified plasmids were then transformed into *E. coli* BL21(DE3) bacteria for protein production.

Chlamydial Transformation: The protocol followed was a modification of the method developed by Mueller and Fields (76). For transformation, 10^6 *C. trachomatis* serovar L2 EBs (25667R) naturally lacking the endogenous plasmid were incubated with 2 µg of unmethylated plasmid in a volume of 50 µL $CaCl_2$ at room temperature for 30 minutes. Each reaction was sufficient for a confluent monolayer of McCoy cells in one well of a six well plate that had been plated a day prior. The transformants were added to a 1 mL overlay of room temperature HBSS per well, and an additional 1 mL of HBSS was then added to each well. The plate was centrifuged at 400 xg for 15 min at room

temperature, where the beginning of this step was recorded as the time of infection. Following the spin, the plate was incubated for 15 minutes at 37° C. This infection was recorded as T_0. The inoculum was aspirated at the end of the incubation and replaced with antibiotic-free DMEM+10% FBS. 8 hours post-infection, the media was replaced with DMEM containing 1 μg/mL cycloheximide, 10 μg/mL gentamicin, and 1 U/mL penicillin. Cells infected with transformants were passaged every 48 hours until a population of penicillin resistant bacteria was established. These EBs were then harvested and frozen in sucrose/phosphate (2SP; (66)) solution at -80° C prior to titration.

Determining the Effect of Overexpression of Clp Mutant Proteins via Immunofluorescence Analysis: Transformed *C. trachomatis* containing a mutant *clp* gene under control of an anhydrotetracycline (aTc) inducible promoter was used to infect a monolayer of HEp2 cells on coverslips with penicillin as a selection agent. Samples were induced with increasing, subtoxic amounts of aTc at 8 hours post-infection and were methanol fixed after either a 6 hour or 14 hour pulse (16 or 24 hours post-infection). Fixed cells were incubated with an anti-Ctr serovar L2 guinea pig primary antibody (kindly provided by Dr. Rucks, UNMC) to stain for the organism and a goat anti-guinea pig Alexa488 conjugated secondary antibody for visualization of organisms within the inclusion. Additionally, a mouse anti-6xHis tag was used, followed by a goat anti-mouse Alexa594 secondary antibody for confirmation of protein expression and localization. Finally, the samples were stained with DAPI to visualize the host cell and bacterial DNA. Representative images were taken on a Zeiss Fluoview1000 laser scanning confocal microscope with a 60x objective and 2x digital zoom and were equally color corrected using Adobe Photoshop CC.

Determining Protein-Protein Interactions with the BACTH System: To test interaction of the Clp proteins, the Bacterial Adenylate Cyclase Two-Hybrid (BACTH) assay was utilized. This assay

relies on reconstitution of adenylate cyclase activity in adenylate cyclase deficient (Δ*cya*) DHT1 *E. coli*. The genes of interest are translationally fused to one of either subunit, denoted as T18 and T25, of the *B. pertussis* adenylate cyclase toxin. Each *clpP* gene cloned into one of the pST25, pSNT25, or pUT18C Gateway® vectors was tested for both homotypic and heterotypic interactions (10). One plasmid from the T25 background and one from the T18 background were co-transformed into the DHT1 $CaCl_2$ competent *E. coli* and were plated on a double antibiotic minimal M63 medium selection plate supplemented with 0.5 mM IPTG for induction of the protein, 40 μg/mL Xgal to give a visual readout upon cleavage, and 0.2% maltose as a unique carbon source. These plates also contain 0.04% casein hydrolysate to supplement the bacteria with the branched chain amino acids as Δ*cya* DHT1 *E. coli* cannot synthesize these amino acids. Blue colonies were indicative of positive interaction between proteins since both the *lac* and *mal* operons require reconstituted cAMP production from interacting T25 and T18 fragments to be expressed. Leucine zipper motifs were used for controls in pKT25 and pUT18C backgrounds on the appropriate antibiotic selection plates because these have been previously shown to interact (77). β-galactosidase activity was then measured from 8 colonies to quantify protein interactions. Random positive colonies were used to inoculate individual wells and grown 24 hours at 30° in M63 with 0.2% maltose and appropriate antibiotics. These bacteria were permeabilized with 0.1% SDS and chloroform prior to addition of 0.1% o-nitrophenol-β-galactoside (ONPG). The reaction was stopped using 1 M $NaHCO_3$ after precisely 20 minutes of incubation at room temperature. Absorbance at the 405 wavelength was recorded and normalized to bacterial growth (OD_{600}), dilution factor, and time (in minutes) of incubation prior to stopping the reaction. Totals were reported in relative units (RU) of β-galactosidase activity.

Purification of Recombinant ClpP1 and ClpP2: His-tagged Ctr ClpP1, Ctr ClpP2, and Ec ClpP were purified from 500 mL cultures of BL21(DE3) *E. coli* transformed with the respective plasmid based on the protocol described in (78). Samples were induced with 0.5 mM IPTG and incubated with shaking for 20 hours at 18°C. Cultures were pelleted and frozen at -20°C prior to purifications. Buffers used are listed in Table S2. Samples were suspended, sonicated, bound to HisPur Cobalt Resin (Thermo Scientific), and washed in buffer A. Proteins were eluted from the resin using buffer B. Buffer exchange for buffer C was performed using a Millipore Amicon Ultra 15 filtration units (3 kDa cut-off). ClpP proteins were quantified using the Bio-Rad Protein assay, assessed for purity on 12% SDS-PAGE gels with Coomassie staining, and identified using anti-His-tag western blot. Blotting was performed using a mouse monoclonal anti-6x His antibody (1:1000; Millipore HIS.H8) and a goat anti-mouse IgG HRP conjugated secondary antibody (1:2000). Protein samples were aliquoted and stored at -80°C.

In Vitro *Analysis of ClpP1 and ClpP2 Homo-Oligomerization:* 5 μg of purified protein was incubated in buffer D at 37°C for 1 hour before being mixed with a 5x native sample buffer (5 mM Tris [pH 6.8], 38 mM glycine, 0.06% bromophenol blue) and analyzed on a BioRad MiniProtean 4-20% gradient gel for Native-PAGE. Samples were run for 90 minutes at 200V. Gels were assessed using Coomassie staining.

***Assessment of ClpP activity* in vitro.** Fluorometric peptide assay: The ClpPs (at 1 μM) were added to 500 μM of Suc-Luc-Tyr-AMC (Boston Biochem) dissolved in buffer E (50 mM Tris-HCl [pH 8], 200 mM KCl, and 1 mM DTT) or buffer F (with 0.2 M sodium citrate) (44). Final reaction volumes were 50 μl. Reactions were monitored over six hours at 37 °C using a BioTek Synergy HT plate reader set at an excitation of 340/360 and an emission of 440/460 with readings taken at five-minute

intervals. Casein degradation assays: Casein (Sigma-Aldrich) was dissolved in buffer E and 1 µg was used per assay. Samples containing casein and 1 µM of the respective ClpP were incubated at 37 °C for 3 hours with or without the respective ACP compound (500 µM). Reactions were halted by mixing with 2x Laemmli buffer containing β-mercaptoethanol and heating at 90-100 °C for 5 minutes. Samples were analyzed for digestion of casein using 12% SDS-PAGE gels followed by Coomassie staining.

Effect of ACP compounds on chlamydial growth and host cell viability. Antibiotic stocks of ACP1, ACP1a, and ACP1b were synthesized (47), resuspended at 25 mg/mL in DMSO, and frozen at -20°C. Methods for the synthesis, purification, and analysis of these compounds is available in Supplementary Information. For assessment of cell viability upon treatment, four wells of a 96 well plate with a confluent monolayer of HEp2 cells were either infected with density gradient purified wild type *C. trachomatis* serovar L2 with an MOI of 1 or left uninfected. These wells were either treated or not with 25 or 50 µg/mL of ACP1, ACP1a, or ACP1b, with a set of DMSO only samples used as a control. Antibiotics were added eight hours post-infection (hpi). At 24 hpi, 100 µL of 2x Resazurin (Abcam) was added to three wells of each treatment condition, adding only DMEM to the fourth as a background control. Following a four-hour incubation at 37º C, absorbance at the 570 nm wavelength was recorded using a Tecan plate reader. The wells were averaged, subtracting background absorbance from samples without dye. Absorbance was reported as percentage of the untreated samples. To quantify the effect of the drug on *C. trachomatis*, variable treatments of each drug (25 µg and 50 µg) were added or not eight hours post-infection. Cell lysates containing *C. trachomatis* were collected in 2SP and frozen at -80° C prior to serial titration on a fresh cell layer. Inclusion forming units (IFUs), a proxy for recoverable EBs from the initial infection samples, were

calculated from the average number of inclusions in 15 fields of view multiplied by the number of fields of view within the well and corrected for the dilution factor and volume of inoculum.

Acknowledgements

We would like to thank Dr. Elizabeth Rucks of UNMC for providing us with multiple antibodies for analysis by immunofluorescence, and for thoughtful review of the manuscript. We thank Dr. Walid Houry (Univ. of Toronto) for providing us with an initial sample of the ACP1b antibiotic, Dr. Tania Baker (MIT) for providing us with Pa_ClpP specific antibodies for use in our experiments, and Dr. H. Caldwell (NIH/NIAID) for eukaryotic cell lines. We also thank Amanda Blocker (SIUC) for providing assistance with protein purification and activity assays. Funding for this project was supported by an NSF CAREER award (1810599) to SPO and University funds to DJF. This project was also funded by the Department of Defense office of the Congressionally Directed Medical Research Programs (CDMRP), 2017 Peer Reviewed Medical Research Program (PRMRP) Discovery Award (PR172445) to MCS.

References:

1. WHO. 2017. Trachoma. http://www.who.int/mediacentre/factsheets/fs382/en/. Accessed
2. Hafner LM, Wilson DP, Timms P. 2014. Development status and future prospects for a vaccine against *Chlamydia trachomatis* infection. Vaccine 32:1563-1571.
3. CDC. 2017. 2017 Sexually Transmitted Diseases Surveillance. https://www.cdc.gov/std/stats16/chlamydia.htm#foot-1. Accessed
4. AbdelRahman YM, Belland RJ. 2006. The chlamydial developmental cycle. FEMS Microbiology Reviews 29:949-959.
5. Hackstadt T, Baehr W, Ying Y. 1991. *Chlamydia trachomatis* developmentally regulated protein is homologous to eukaryotic histone H1. Proceedings of the National Academy of Sciences of the United States of America 88:3937-3941.
6. Hatch TP, Allan I, Pearce JH. 1984. Structural and polypeptide differences between envelopes of infective and reproductive life cycle forms of *Chlamydia* spp. Journal of Bacteriology 157:13-20.
7. Clifton DR, Fields KA, Grieshaber SS, Dooley CA, Fischer ER, Mead DJ, Carabeo RA, Hackstadt T. 2004. A chlamydial type III translocated protein is tyrosine-phosphorylated at the site of entry and associated with recruitment of actin. Proceedings of the National Academy of Sciences of the United States of America 101:10166.
8. Lane BJ, Mutchler C, Al Khodor S, Grieshaber SS, Carabeo RA. 2008. Chlamydial Entry Involves TARP Binding of Guanine Nucleotide Exchange Factors. PLoS Pathogens 4:e1000014.
9. Hodinka RL, Davis CH, Choong J, Wyrick PB. 1988. Ultrastructural study of endocytosis of *Chlamydia trachomatis* by McCoy cells. Infection and Immunity 56:1456-1463.

10. Moore ER, Ouellette SP. 2014. Reconceptualizing the chlamydial inclusion as a pathogen-specified parasitic organelle: an expanded role for Inc proteins. Frontiers in Cellular and Infection Microbiology 4:157.

11. Belland RJ, Zhong G, Crane DD, Hogan D, Sturdevant D, Sharma J, Beatty WL, Caldwell HD. 2003. Genomic transcriptional profiling of the developmental cycle of *Chlamydia trachomatis*. Proceedings of the National Academy of Sciences of the United States of America 100:8478-8483.

12. Vandahl BBS, Birkelund S, Christiansen G. 2004. Genome and proteome analysis of Chlamydia. PROTEOMICS 4:2831-2842.

13. Skipp PJS, Hughes C, McKenna T, Edwards R, Langridge J, Thomson NR, Clarke IN. 2016. Quantitative Proteomics of the Infectious and Replicative Forms of Chlamydia trachomatis. PLoS ONE 11:e0149011.

14. Saka HA, Thompson JW, Chen Y-S, Kumar Y, Dubois LG, Moseley MA, Valdivia RH. 2011. Quantitative proteomics reveals metabolic and pathogenic properties of Chlamydia trachomatis developmental forms. Molecular Microbiology 82:1185-1203.

15. Beatty WL, Byrne GI, Morrison RP. 1993. Morphologic and antigenic characterization of interferon gamma-mediated persistent Chlamydia trachomatis infection in vitro. Proceedings of the National Academy of Sciences of the United States of America 90:3998-4002.

16. Raulston JE. 1997. Response of Chlamydia trachomatis serovar E to iron restriction in vitro and evidence for iron-regulated chlamydial proteins. Infection and Immunity 65:4539-4547.

17. Matsumoto A, Manire GP. 1970. Electron Microscopic Observations on the Effects of Penicillin on the Morphology of Chlamydia psittaci. Journal of Bacteriology 101:278-285.

18. Stephens RS, Kalman S, Lammel C, Fan J, Marathe R, Aravind L, Mitchell W, Olinger L, Tatusov RL, Zhao Q, Koonin EV, Davis RW. 1998. Genome Sequence of an Obligate Intracellular Pathogen of Humans: *Chlamydia trachomatis*. Science 282:754.

19. Stinson BM, Nager AR, Glynn SE, Schmitz KR, Baker TA, Sauer RT. 2013. Nucleotide binding and conformational switching in the hexameric ring of a AAA+ machine. Cell 153:628-639.

20. Kirstein J, Schlothauer T, Dougan DA, Lilie H, Tischendorf G, Mogk A, Bukau B, Turgay K. 2006. Adaptor protein controlled oligomerization activates the AAA+ protein ClpC. The EMBO Journal 25:1481-1491.

21. Baker TA, Sauer RT. 2012. ClpXP, an ATP-powered unfolding and protein-degradation machine. Biochimica et biophysica acta 1823:15-28.

22. Alexopoulos JA, Guarné A, Ortega J. 2012. ClpP: A structurally dynamic protease regulated by AAA+ proteins. Journal of Structural Biology 179:202-210.

23. Yu AYH, Houry WA. 2007. ClpP: A distinctive family of cylindrical energy-dependent serine proteases. FEBS Letters 581:3749-3757.

24. Grimaud R, Kessel M, Beuron F, Steven AC, Maurizi MR. 1998. Enzymatic and Structural Similarities between the *Escherichia coli* ATP-dependent Proteases, ClpXP and ClpAP. Journal of Biological Chemistry 273:12476-12481.

25. Bewley MC, Graziano V, Griffin K, Flanagan JM. 2006. The asymmetry in the mature amino-terminus of ClpP facilitates a local symmetry match in ClpAP and ClpXP complexes. Journal of structural biology 153:113-128.

26. Hall BM, Breidenstein EBM, de la Fuente-Núñez C, Reffuveille F, Mawla GD, Hancock REW, Baker TA. 2017. Two Isoforms of Clp Peptidase in *Pseudomonas aeruginosa* Control Distinct Aspects of Cellular Physiology. Journal of Bacteriology 199:e00568-16.

27. Akopian T, Kandror O, Raju RM, UnniKrishnan M, Rubin EJ, Goldberg AL. 2012. The active ClpP protease from *M. tuberculosis* is a complex composed of a heptameric ClpP1 and a ClpP2 ring. The EMBO Journal 31:1529-1541.

28. Dahmen M, Vielberg M-T, Groll M, Sieber Stephan A. 2015. Structure and Mechanism of the Caseinolytic Protease ClpP1/2 Heterocomplex from Listeria monocytogenes. Angewandte Chemie International Edition 54:3598-3602.

29. Balogh D, Dahmen M, Stahl M, Poreba M, Gersch M, Drag M, Sieber SA. 2017. Insights into ClpXP proteolysis: heterooligomerization and partial deactivation enhance chaperone affinity and substrate turnover in *Listeria monocytogenes*. Chemical Science 8:1592-1600.

30. Shaw EI, Dooley CA, Fischer ER, Scidmore MA, Fields KA, Hackstadt T. 2002. Three temporal classes of gene expression during the *Chlamydia trachomatis* developmental cycle. Molecular Microbiology 37:913-925.

31. Wichlan DG, Hatch TP. 1993. Identification of an early-stage gene of *Chlamydia psittaci* 6BC. Journal of Bacteriology 175:2936-2942.

32. Douglas AL, Hatch TP. 2000. Expression of the transcripts of the sigma factors and putative sigma factor regulators of *Chlamydia trachomatis L2*. Gene 247:209-214.

33. Ouellette SP, Rueden KJ, Gauliard E, Persons L, de Boer PA, Ladant D. 2014. Analysis of MreB interactors in Chlamydia reveals a RodZ homolog but fails to detect an interaction with MraY. Frontiers in Microbiology 5:279.

34. Martin A, Baker TA, Sauer RT. 2008. Diverse pore loops of the AAA+ ClpX machine mediate unassisted and adaptor-dependent recognition of ssrA-tagged substrates. Molecular cell 29:441-450.

35. Ni T, Ye F, Liu X, Zhang J, Liu H, Li J, Zhang Y, Sun Y, Wang M, Luo C, Jiang H, Lan L, Gan J, Zhang A, Zhou H, Yang C-G. 2016. Characterization of Gain-of-Function Mutant Provides New Insights into ClpP Structure. ACS Chemical Biology 11:1964-1972.

36. Wickstrum J, Sammons LR, Restivo KN, Hefty PS. 2013. Conditional Gene Expression in *Chlamydia trachomatis* Using the Tet System. PLoS ONE 8:e76743.

37. Ouellette SP. 2018. Feasibility of a Conditional Knockout System for *Chlamydia* Based on CRISPR Interference. Frontiers in Cellular and Infection Microbiology 8:59.

38. Feng J, Michalik S, Varming AN, Andersen JH, Albrecht D, Jelsbak L, Krieger S, Ohlsen K, Hecker M, Gerth U, Ingmer H, Frees D. 2013. Trapping and Proteomic Identification of Cellular Substrates of the ClpP Protease in *Staphylococcus aureus*. Journal of Proteome Research 12:547-558.

39. Rucks EA, Olson MG, Jorgenson LM, Srinivasan RR, Ouellette SP. 2017. Development of a Proximity Labeling System to Map the Chlamydia trachomatis Inclusion Membrane. Frontiers in Cellular and Infection Microbiology 7:40.

40. Joshi SA, Hersch GL, Baker TA, Sauer RT. 2004. Communication between ClpX and ClpP during substrate processing and degradation. Nature Structural &Amp; Molecular Biology 11:404.

41. Schmitz KR, Carney DW, Sello JK, Sauer RT. 2014. Crystal structure of *Mycobacterium tuberculosis* ClpP1P2 suggests a model for peptidase activation by AAA+ partner binding and substrate delivery. Proceedings of the National Academy of Sciences of the United States of America 111:E4587-E4595.

42. Karimova G, Pidoux J, Ullmann A, Ladant D. 1998. A bacterial two-hybrid system based on a reconstituted signal transduction pathway. Proceedings of the National Academy of Sciences of the United States of America 95:5752-5756.

43. Woo KM, Chung WJ, Ha DB, Goldberg AL, Chung CH. 1989. Protease Ti from Escherichia coli requires ATP hydrolysis for protein breakdown but not for hydrolysis of small peptides. Journal of Biological Chemistry 264:2088-2091.

44. Gersch M, Stahl M, Poreba M, Dahmen M, Dziedzic A, Drag M, Sieber SA. 2016. Barrel-shaped ClpP Proteases Display Attenuated Cleavage Specificities. ACS Chemical Biology 11:389-399.

45. Brötz-Oesterhelt H, Beyer D, Kroll H-P, Endermann R, Ladel C, Schroeder W, Hinzen B, Raddatz S, Paulsen H, Henninger K, Bandow JE, Sahl H-G, Labischinski H. 2005. Dysregulation of bacterial proteolytic machinery by a new class of antibiotics. Nature Medicine 11:1082.

46. Conlon BP, Nakayasu ES, Fleck LE, LaFleur MD, Isabella VM, Coleman K, Leonard SN, Smith RD, Adkins JN, Lewis K. 2013. Killing persister cells and eradicating a biofilm infection by activating the ClpP protease. Nature 503:365-370.

47. Leung E, Datti A, Cossette M, Goodreid J, McCaw Shannon E, Mah M, Nakhamchik A, Ogata K, El Bakkouri M, Cheng Y-Q, Wodak Shoshana J, Eger Bryan T, Pai Emil F, Liu J, Gray-Owen S, Batey Robert A, Houry Walid A. 2011. Activators of Cylindrical Proteases as Antimicrobials: Identification and Development of Small Molecule Activators of ClpP Protease. Chemistry & Biology 18:1167-1178.

48. Hwang BJ, Park WJ, Chung CH, Goldberg AL. 1987. *Escherichia coli* contains a soluble ATP-dependent protease (Ti) distinct from protease La. Proceedings of the National Academy of Sciences of the United States of America 84:5550-5554.

49. Flanagan JM, Wall JS, Capel MS, Schneider DK, Shanklin J. 1995. Scanning Transmission Electron Microscopy and Small-Angle Scattering Provide Evidence that Native *Escherichia coli* ClpP is a Tetradecamer with an Axial Pore. Biochemistry 34:10910-10917.

50. Wang J, Hartling JA, Flanagan JM. 1997. The Structure of ClpP at 2.3 Å Resolution Suggests a Model for ATP-Dependent Proteolysis. Cell 91:447-456.

51. Lee ME, Baker TA, Sauer RT. 2010. Control of substrate gating and translocation into ClpP by channel residues and ClpX binding. Journal of molecular biology 399:707-718.

52. Thompson MW, Singh SK, Maurizi MR. 1994. Processive degradation of proteins by the ATP-dependent Clp protease from *Escherichia coli*. Requirement for the multiple array of active sites in ClpP but not ATP hydrolysis. Journal of Biological Chemistry 269:18209-18215.

53. Jennings LD, Bohon J, Chance MR, Licht S. 2008. The ClpP N-terminus coordinates substrate access with protease active site reactivity. Biochemistry 47:11031-11040.

54. Benaroudj N, Raynal B, Miot M, Ortiz-Lombardia M. 2011. Assembly and proteolytic processing of mycobacterial ClpP1 and ClpP2. BMC Biochemistry 12:61-61.

55. Dahmen M, Vielberg MT, Groll M, Sieber Stephan A. 2015. Structure and Mechanism of the Caseinolytic Protease ClpP1/2 Heterocomplex from *Listeria monocytogenes*. Angewandte Chemie International Edition 54:3598-3602.

56. Gaillot O, Bregenholt S, Jaubert F, Di Santo JP, Berche P. 2001. Stress-Induced ClpP Serine Protease of *Listeria monocytogenes* Is Essential for Induction of Listeriolysin O-Dependent Protective Immunity. Infection and Immunity 69:4938-4943.

57. Martin A, Baker TA, Sauer RT. 2007. Distinct static and dynamic interactions control ATPase-peptidase communication in a AAA+ protease. Molecular cell 27:41-52.

58. Lee B-G, Park EY, Lee K-E, Jeon H, Sung KH, Paulsen H, Rübsamen-Schaeff H, Brötz-Oesterhelt H, Song HK. 2010. Structures of ClpP in complex with acyldepsipeptide antibiotics reveal its activation mechanism. Nature Structural &Amp; Molecular Biology 17:471.

59. Bewley MC, Graziano V, Griffin K, Flanagan JM. 2009. Turned on for degradation: ATPase-independent degradation by ClpP. Journal of structural biology 165:118-125.

60. Li DHS, Chung YS, Gloyd M, Joseph E, Ghirlando R, Wright GD, Cheng Y-Q, Maurizi MR, Guarné A, Ortega J. 2010. Acyldepsipeptide Antibiotics Induces the Formation of a Structured Axial Channel in ClpP: a Model for the ClpX/ClpA Bound State of ClpP. Chemistry & biology 17:959-969.

61. Ouellette SP, Dorsey FC, Moshiach S, Cleveland JL, Carabeo RA. 2011. Chlamydia Species-Dependent Differences in the Growth Requirement for Lysosomes. PLoS ONE 6:e16783.

62. Lutz R, Bujard H. 1997. Independent and tight regulation of transcriptional units in Escherichia coli via the LacR/O, the TetR/O and AraC/I1-I2 regulatory elements. Nucleic Acids Research 25:1203-1210.

63. Wang B, Barahona M, Buck M. 2015. Amplification of small molecule-inducible gene expression via tuning of intracellular receptor densities. Nucleic Acids Research 43:1955-1964.

64. Kane CD, Vena RM, Ouellette SP, Byrne GI. 1999. Intracellular Tryptophan Pool Sizes May Account for Differences in Gamma Interferon-Mediated Inhibition and Persistence of Chlamydial Growth in Polarized and Nonpolarized Cells. Infection and Immunity 67:1666-1671.

65. Ouellette SP, Rueden KJ, Rucks EA. 2016. Tryptophan Codon-Dependent Transcription in Chlamydia pneumoniae during Gamma Interferon-Mediated Tryptophan Limitation. Infection and Immunity 84:2703-2713.

66. Wang Y, Kahane S, Cutcliffe LT, Skilton RJ, Lambden PR, Clarke IN. 2011. Development of a Transformation System for *Chlamydia trachomatis*: Restoration of Glycogen Biosynthesis by Acquisition of a Plasmid Shuttle Vector. PLoS Pathogens 7:e1002258.

67. Illingworth M, Hooppaw AJ, Ruan L, Fisher DJ, Chen L. 2017. Biochemical and Genetic Analysis of the Chlamydia GroEL Chaperonins. Journal of Bacteriology 199:e00844-16.

68. Scidmore MA. 2006. Cultivation and Laboratory Maintenance of Chlamydia trachomatis. Current Protocols in Microbiology 00:11A.1.1-11A.1.25.

69. Altschul SF, Wootton JC, Gertz EM, Agarwala R, Morgulis A, Schäffer AA, Yu Y-K. 2005. Protein Database Searches Using Compositionally Adjusted Substitution Matrices. The FEBS journal 272:5101-5109.

70. Sievers F, Wilm A, Dineen D, Gibson TJ, Karplus K, Li W, Lopez R, McWilliam H, Remmert M, Söding J, Thompson JD, Higgins DG. 2011. Fast, scalable generation of high-quality protein multiple sequence alignments using Clustal Omega. Molecular Systems Biology 7:539-539.

71. Troshin PV, Procter JB, Barton GJ. 2011. Java bioinformatics analysis web services for multiple sequence alignment—JABAWS:MSA. Bioinformatics 27:2001-2002.

72. Kelley LA, Mezulis S, Yates CM, Wass MN, Sternberg MJE. 2015. The Phyre2 web portal for protein modelling, prediction and analysis. Nature protocols 10:845-858.

73. Pettersen EF, Goddard TD, Huang CC, Couch GS, Greenblatt DM, Meng EC, Ferrin TE. 2004. UCSF Chimera—A visualization system for exploratory research and analysis. Journal of Computational Chemistry 25:1605-1612.

74. Ouellette SP, Gauliard E, Antosová Z, Ladant D. 2014. A Gateway®-compatible bacterial adenylate cyclase-based two-hybrid system. Environmental Microbiology Reports 6:259-267.

75. Ouellette SP, Hatch TP, AbdelRahman YM, Rose LA, Belland RJ, Byrne GI. 2006. Global transcriptional upregulation in the absence of increased translation in Chlamydia during IFNγ-mediated host cell tryptophan starvation. Molecular Microbiology 62:1387-1401.

76. Mueller KE, Wolf K, Fields KA. 2017. Chlamydia trachomatis Transformation and Allelic Exchange Mutagenesis. Current Protocols in Microbiology 45:11A.3.1-11A.3.15.

77. Robichon C, Karimova G, Beckwith J, Ladant D. 2011. Role of Leucine Zipper Motifs in Association of the *Escherichia coli* Cell Division Proteins FtsL and FtsB. Journal of Bacteriology 193:4988-4992.

78. Trentini DB, Suskiewicz MJ, Heuck A, Kurzbauer R, Deszcz L, Mechtler K, Clausen T. 2016. Arginine phosphorylation marks proteins for degradation by a Clp protease. Nature 539:48.

Figure Legends

Figure 1: The *clp* genes are transcribed, and ClpP2 is produced, during RB growth. (A) Gene maps of the *clp* genes in the *Chlamydia trachomatis* genome. Gene numbers are in numerical order from left to right and reflect the serovar D numbering scheme of Stephens et al. (18). The *clp* genes are circled in red. The *clpP2* gene is *ct706*. **(B) RT-qPCR** analysis of the *clp* genes from two independent time course experiments of a *C. trachomatis* serovar L2 infection of HEp2 cells. Total RNA and DNA were collected at the indicated times post infection and processed as described in Materials and Methods. Equivalent amounts of cDNA were used for each assay and analyzed in triplicate. Results were reported as a ratio of cDNA to genomic DNA. Standard deviations for each were typically less than 10% of the sample. Note that some transcripts were not detectable at 1 hpi. **Temporal expression** of **(C)** ClpP2, using a *Pseudomonas aeruginosa* ClpP1-specific antibody, and **(D)** the chlamydial major outer membrane protein (MOMP) was assessed. Whole cell lysates of total protein from a time course of *Chlamydia*-infected cells **(E)** were separated by SDS-PAGE and transferred to a PVDF membrane for blotting.

Figure 2: Bioinformatics analyses suggest both chlamydial ClpP paralogs are functional proteases. (A) Pairwise alignments performed using NCBI-BLAST (default settings) and presented as %Identity/%Similarity/%Coverage. Multiple sequence alignment performed using Clustal Omega default settings and presented using Jalview Version 2. Organisms included are *C. trachomatis* (Ctr), *Escherichia coli* (Ec), *Bacillus subtilis* (Bs), *Mycobacterium tuberculosis* (Mtb), and *Pseudomonas aeruginosa* (Pa). Conserved residues highlighted in varying shades of blue depending on conservation strength across species, with the catalytic triad in red, the oligomer interface in yellow, and the hydrophobic docking region in green. Residues in which ClpP1 has a different substitution

compared to other ClpP proteins are denoted by Ω. Residues involved in activation conformational changes denoted by ψ (35) **(B)** Predicted 3D structures of Ctr ClpP1, Ctr ClpP2, and Ec ClpP (peptide colors as shown in multiple sequence alignment) acquired from Phyre2 and aligned and colored in Chimera (UCSF). Active site residues are circled in red. **(C) Space filling model** of predicted 3D structures as in (B). "Rear" is a 180° rotation around the Y axis to show the surface of the protein not shown in the "Front" image. The active site is again circled in red.

Figure 3: Over-expression of inactive ClpP1, but not ClpP2, inhibits chlamydial inclusion growth. *C. trachomatis* serovar L2 was transformed with anhydrotetracycline (aTc)-inducible shuttle vectors encoding active site mutants of each ClpP paralog with a 6xHis tag at the C-terminus. HEp2 cells were infected with each transformant, and expression of the inactive ClpP_6xHis was induced at 10h post infection (hpi). **(A) ClpP1(S92A) overexpression** assay. Overexpression of inactive ClpP1 has a negative impact on inclusion growth. **(B) ClpP2(S98A) overexpression** assay. Parameters same as described above. Overexpression does not appear to negatively affect *Chlamydia*. For (A) and (B), samples were stained for major outer membrane protein (CtrL2; green), 6xHis tagged ClpP protein of interest (red), and DNA (blue) with a composite image of all channels merged (Merge). Representative images of three independent experiments are presented. Scale bars are equal to 10 μm. Images were acquired on a Fluoview1000 laser scanning confocal microscope with a 60x objective and a 2x digital magnification.

Figure 4: The chlamydial ClpP paralogs self-associate but do not form hetero-oligomeric complexes. (A) Bacterial adenylate cyclase-based two-hybrid assay of homotypic interactions of *C. trachomatis* (Ctr) ClpP1 and ClpP2. The indicated constructs encoding each *clpP* paralog fused to the T18 or T25 fragment of the Cya toxin of *B. pertussis* were co-transformed into Δ*cya E. coli*

DHT1 and plated on minimal medium containing X-gal. Interactions between proteins results in the formation of blue colonies. Representative images of results from at least three independent experiments are shown along with positive (Zip/Zip) and negative (T25 empty vector versus T18-Zip) controls. Photos set to grayscale. **(B) β-Galactosidase assay** results from experiments performed as described in Panel (A). Y-axis is a measurement of relative units of beta-galactosidase activity. X-axis indicates the test conditions. Interactions are considered positive when at least five times the activity of the negative control is measured. Only homotypic interactions were positive in these assays. Note that the inactive mutants of each ClpP also interact homotypically. **(C) Test of ClpP Oligomerization by Native-PAGE**. 5 µg samples were run on 4-20% native-PAGE gels and stained with Coomassie for protein detection. Representative results from at least three experiments with independent protein purifications are shown. The Ctr ClpP1 methionine mutant (M6L/M7I) was run in a separate lane and the contrast was uniformly adjusted to help with band visualization. Native molecular weight markers are shown to the left of the gel. *E. coli* ClpP (Ec ClpP) is included as a positive control on the far right of the gel. **(D) Test of Hetero-oligomerization between Ctr ClpP1 and Ctr ClpP2.** Each recombinant protein was incubated together prior to electrophoresis. The gel has been cropped and enlarged to aid in detecting P1 and P2 hetero-oligomers, which appear to be absent consistent with panel (B) results. The predicted heptamer/tetradecamer sizes in kDa are: Ctr ClpP1, 154/308; Ctr ClpP2 161/322; and Ec ClpP 168/336.

Figure 5: Chlamydial ClpP2, but not ClpP1, has chaperone-independent protease activity. *In vitro* protease activity of the *C. trachomatis* (Ctr) ClpP proteins versus a peptide substrate. ClpP samples (1 µM) were incubated with the fluorometric peptide Suc-Luc-Tyr-AMC, and fluorescence was analyzed over a time. **(A) Relative activity** is shown for each protein assayed with or without the sodium citrate buffer. Use of sodium citrate buffer is indicated as “Sod-Cit”. **(B) Loss of activity**

is observed for the Ctr ClpP2 catalytic serine mutant. **(C) *E. coli* ClpP** (Ec ClpP) was used as a positive control. Experiments were run a minimum of three times and baseline assay values obtained with buffer alone were subtracted from each sample. Average values are reported with standard error.

Figure 6: ClpP2, but not ClpP1, activity is stimulated by the antibiotic ACP1, which is detrimental to chlamydial growth. (A-C) Casein (1 µg) was incubated with 1 µM of the respective ClpP at 37 °C for 3 hours with or without the ACP compounds (used at 500 µM). Reactions were halted by mixing samples with Laemmli followed by boiling. Samples were run on 12% SDS-PAGE and stained with Coomassie. Molecular weight markers are shown to the left of each gel. Representative gels are shown; at least three experiments were performed for each protein. Ctr = *C. trachomatis.* Ec = *E. coli* **(D) Cell viability** of ACP treated cells were analyzed with resazurin assays. Values are reported as a percentage of the vehicle control and are representative of three independent experiments. **(E) Reinfection models** of ACP drug-treated cells reported on a Log_{10} scale. A student's two-tailed T test was used to compare each parameter to the vehicle control (***= $P<0.0001$). For (D) and (E), HEp2 cells were infected with *C. trachomatis* serovar L2, and the ACP1 compounds or DMSO only was added to the infected cultures at 8 hours post-infection (hpi). At 24 hpi, cell viability was assessed for (D), or infected cells were collected to re-infect fresh monolayers to determine the recovery of inclusion forming units (IFUs) as described in Materials and Methods for (E).

A.

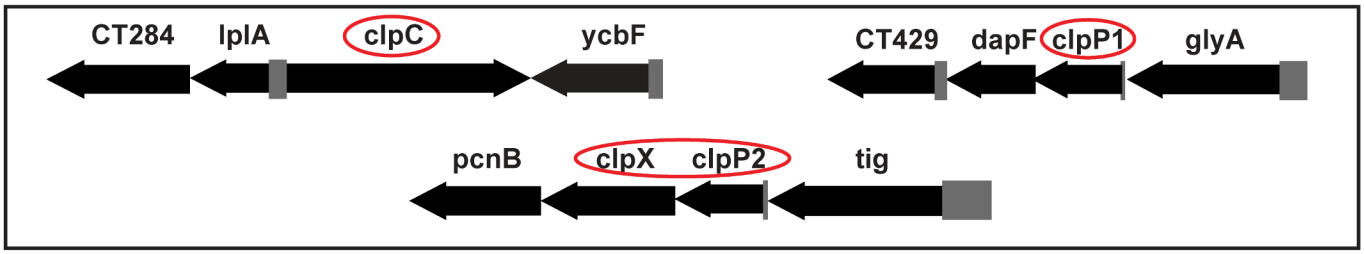

B.

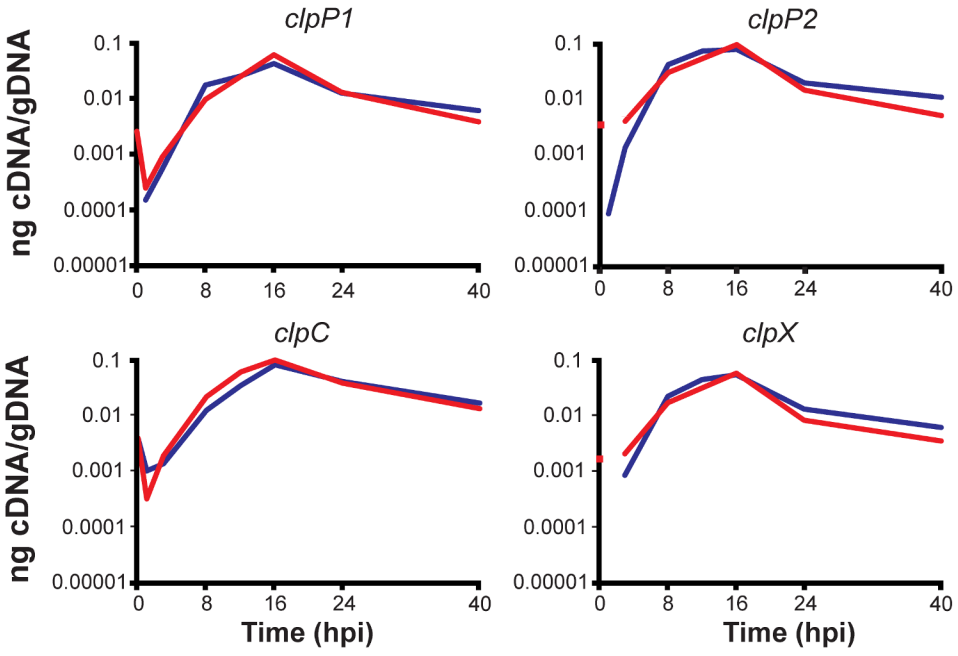

C. Infected Cell Lysates, Anti-ClpP2 1º Ab

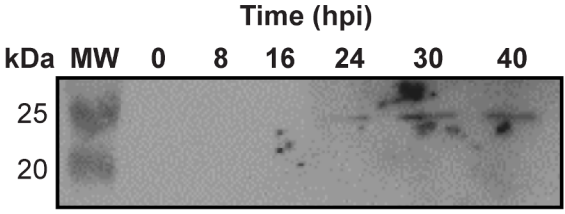

D. Infected Cell Lysates, MOMP 1º Ab

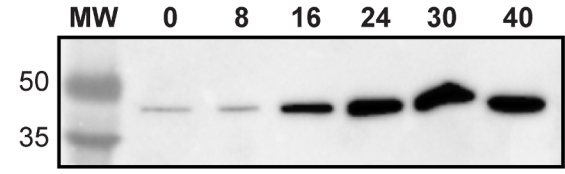

E. Total Protein (Coomassie Stain)

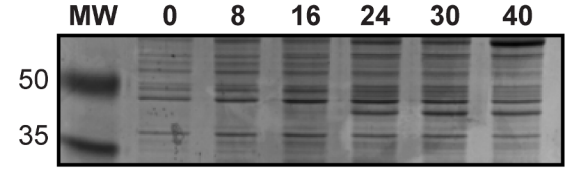

Fig. 1

A.

	Ctr ClpP1	Ctr ClpP2	Ec ClpP	Bs ClpP	Mtb ClpP1	Mtb ClpP2	Pa ClpP1	Pa ClpP2
Ctr ClpP1	-	39%/58%/85%	44%/63%/84%	41%/61%/91%	38%/55%/87%	38%/58%/79%	42%/62%/80%	36%/62%/86%
Ctr ClpP2	39%/58%/91%	-	55%/78%/78%	58%/77%/100%	52%/74%/87%	44%/68%/90%	58%/78%/91%	45%/66%/88%

```
                                                                                                Ψ                                ΨΩ    ΩΩ
Ctr P1   1 ------------------------MPEGEMMHKLQDVIDRKLLDSRRIFFSEPVTEKSAAEAIKKLWYLELTNPGQ  52
Ctr P2   1 -----------------MTLVPYVVEDTGRGERAMDIYSRLLKDRIVMIGQEITEPLANTVIAQLLFLMSEDPTK  58
Ec P     1 ---MSYSGERDNFA-PHMALVPMVIEQTSRGERSFDIYSRLLKERVIFLTGQVEDHMANLIVAQMLFLEAENPEK  71
Bs P     1 -----------------MNLIPTVIEQTNRGERAYDIYSRLLKDRIIMLGSAIDDNVANSIVSQLLFLAAEDPEK  58
Mtb P1   1 -----------------MSQVTDMRSNSQGLSLTDSVYERLLSERIIFLGSEVNDEIANRLCAQILLLAAEDASK  58
Mtb P2   1 -----MNSQNSQIQPQARYILPSFIEHSSFGVKESNPYNKLFEERIIFLGVQVDDASANDIMAQLLVLESLDPDR  70
Pa P1    1 MSRNSFIPHVPDIQ-AAGGLVPMVVEQSARGERAYDIYSRLLKERVIFLVGQVEDYMANLVVAQLLFLEAENPEK  74
Pa P2    1 -----MK-----------TDDKDREGGDSHGAIGAKLMEYALKVRKVFVTGGVDEKMAKDVVQQLHILASI-SDD  58
                Ψ           Ω           Ω
Ctr P1  53 PIVFVINSPGGSVDAGFAVWDQIKMISSPLTTVVTGLAASMGSVLSLCAVPGRRFATPHARIMIHQPSIGGTITG 127
Ctr P2  59 DIQIFINSPGGYITAGLAIYDTIRFLGCDVNTYCIGQAASMGALLLSAGTKGKRYALPHSRMMIHQPS--GGIIG 131
Ec P    72 DIYLYINSPGGVITAGMSIYDTMQFIKPDVSTICMGQAASMGAFLLTAGAKGKRFCLPNSRVMIHQPL--GGYQG 144
Bs P    59 EISLYINSPGGSITAGMAIYDTMQFIKPKVSTICIGMAASMGAFLLAAGEKGKRYALPNSEVMIHQPL--GGAQG 131
Mtb P1  59 DISLYINSPGGSISAGMAIYDTMVLAPCDIATYAMGMAASMGEFLLAAGTKGKRYALPHARILMHQPL--GGVTG 131
Mtb P2  71 DITMYINSPGGGFTSLMAIYDTMQYVRADIQTVCLGQAASAAAVLLAAGTPGKRMALPNARVLIHQPSLSGVIQG 145
Pa P1   75 DIHLYINSPGGSVTAGMSIYDTMQFIKPNVSTTCIGQACSMGALLLAGGAAGKRYCLPHSRMMIHQPL--GGFQG 147
Pa P2   59 PIYMFVNSPGGHVESGDMIFDAIRFITPKVIMIGSGSVASAGALIYAAADKENRYSLPNTRFLLHQPS--GGIQG 131
                                                                Ω
Ctr P1 128 QATDLDIHAREILKTKARIIDVYVEATGQSPEVIEKAIDRDMWMSANEAMEFGLLDGILFSFNDL------- 192
Ctr P2 132 TSADIQLQAAEILTLKKHLSNILAECTGQSVEKIIEDSERDFFMGAEEAIAYGLIDKVISSAKETKDKSIAS 203
Ec P   145 QATDIEIHAREILKVKGRMNELMALHTGQSLEQIERDTERDRFLSAPEAVEYGLVDSILTHRN--------- 207
Bs P   132 QATEIEIAAKRILLLRDKLNKVLAERTGQPLEVIERDTDRDNFKSAEEALEYGLIDKILTHTEDKK------ 197
Mtb P1 132 SAADIAIQAEQFAVIKKEMFRLNAEFTGQPIERIEADSDRDRWFTAAEALEYGFVDHIITRAHVNGEAQ--- 200
Mtb P2 146 QFSDLEIQAAEIERMRTLMETTLARHTGKDAGVIRKDTDRDKILTAEEAKDYGIIDTVLEYRKLSAQTA--- 214
Pa P1  148 QASDIEIHAKEILFIKERLNQILAHHTGQPLDVIARDTDRDRFMSGDEAVKYGLIDKVMTQRDLAV------ 213
Pa P2  132 PASNIEIYRREIVRMKERLDRIFAEATGQTPEKISADTERDFWLNAEEAVQYGLVNKIIVSEREITLPGQ-- 201
```

B.

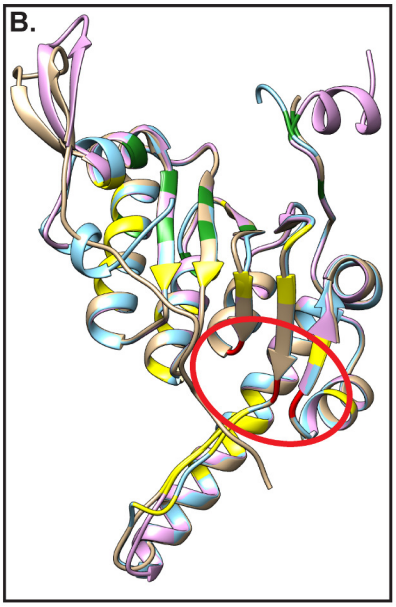

Oligomer Interface
Catalytic Triad
Hydrophobic Docking Site

C.

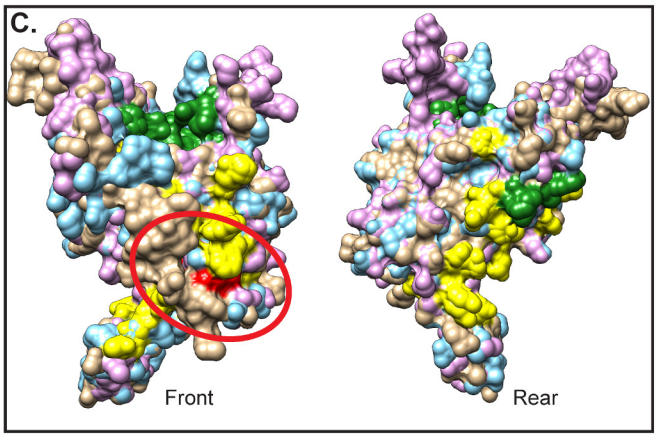

Fig. 2

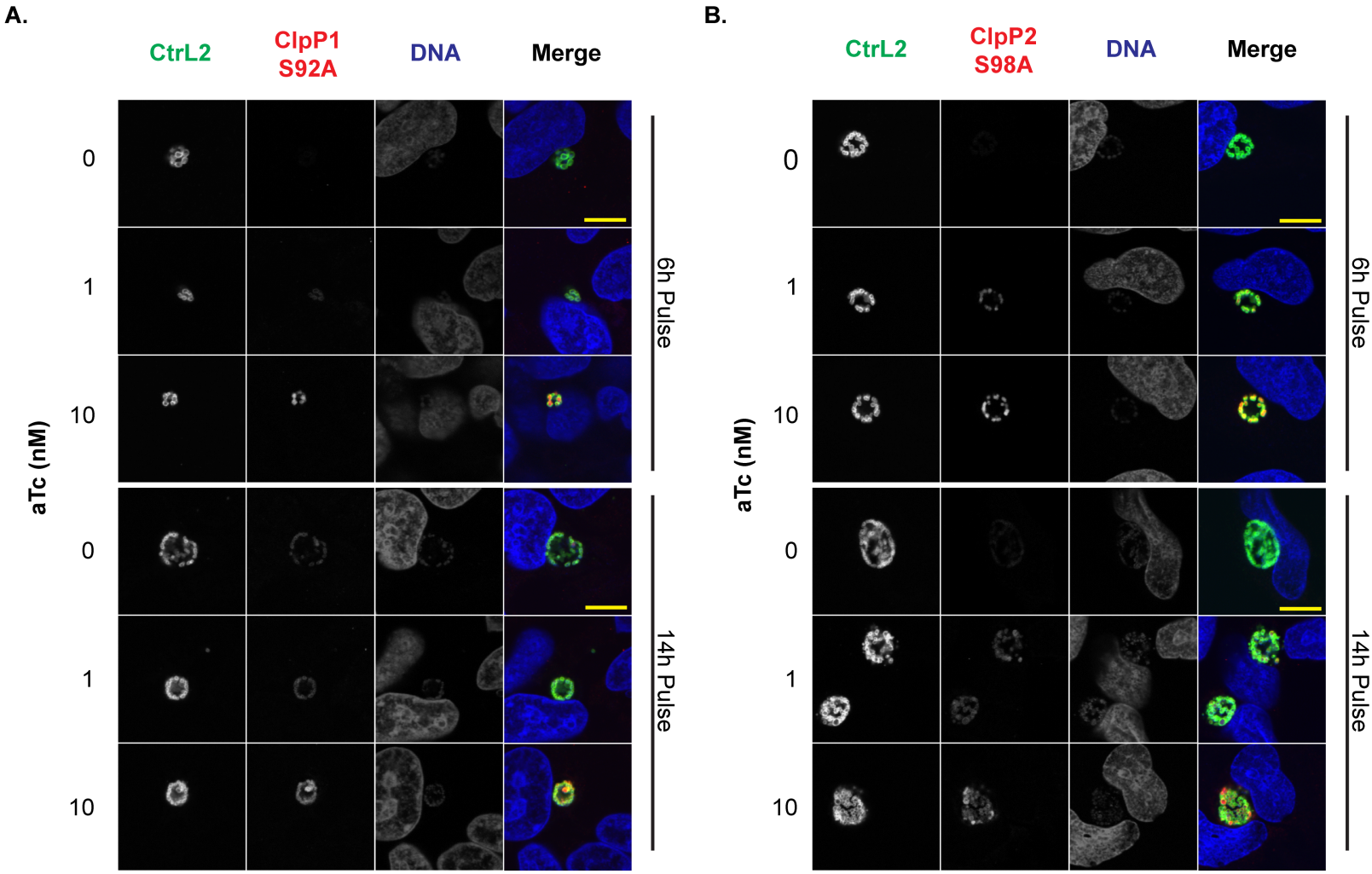
A.
CtrL2
ClpP1 S92A
DNA
Merge
aTc (nM)
0
1
10
0
1
10
6h Pulse
14h Pulse
B.
CtrL2
ClpP2 S98A
DNA
Merge
aTc (nM)
0
1
10
0
1
10
6h Pulse
14h Pulse

Fig. 3

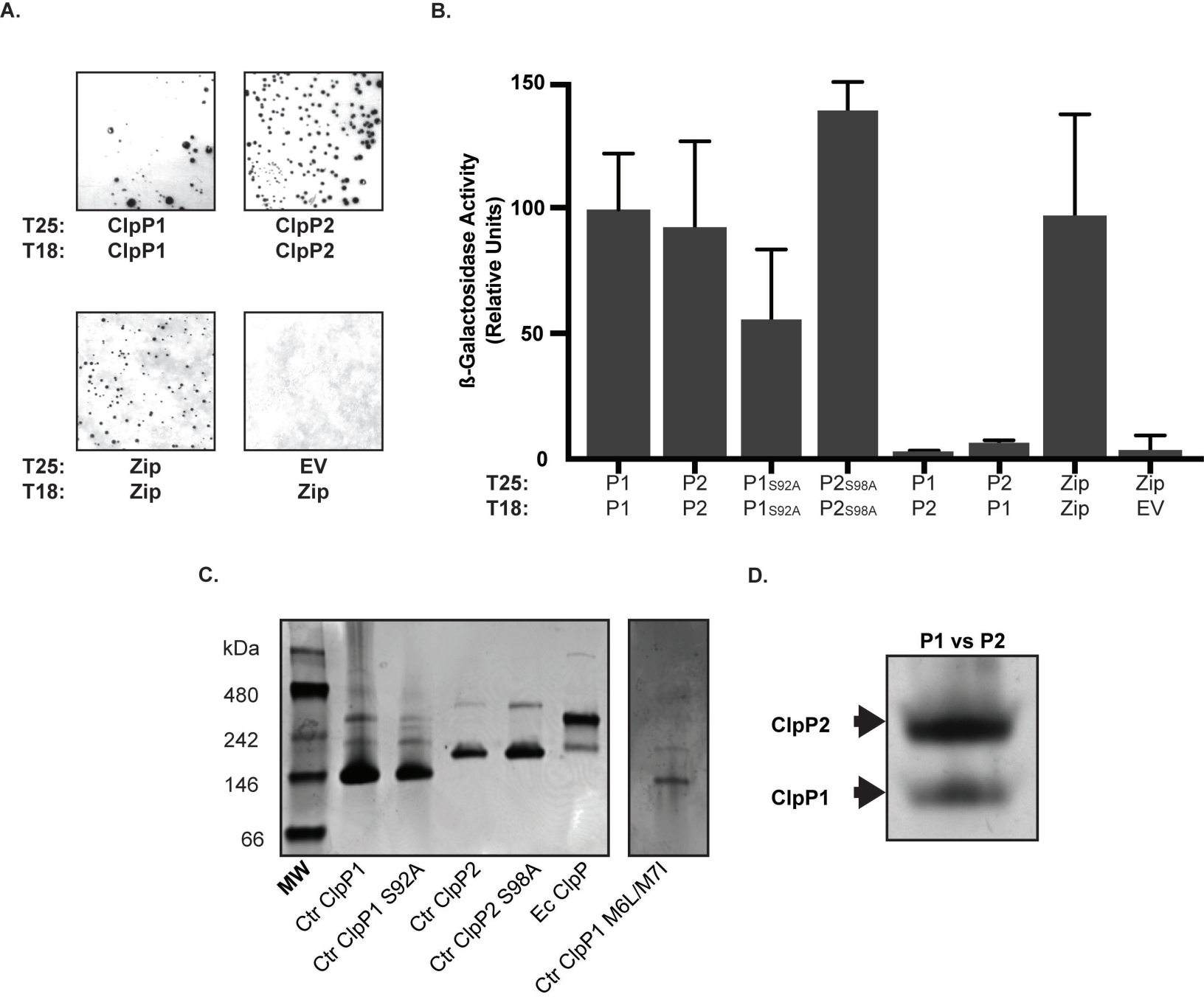
A.
T25: ClpP1
T18: ClpP1
T25: ClpP2
T18: ClpP2
T25: Zip
T18: Zip
T25: EV
T18: Zip
B.
ß-Galactosidase Activity (Relative Units)
150
100
50
0
T25: P1 P2 P1S92A P2S98A P1 P2 Zip Zip
T18: P1 P2 P1S92A P2S98A P2 P1 Zip EV
C.
kDa
480
242
146
66
MW
Ctr ClpP1
Ctr ClpP1 S92A
Ctr ClpP2
Ctr ClpP2 S98A
Ec ClpP
Ctr ClpP1 M6L/M7I
D.
P1 vs P2
ClpP2
ClpP1

Fig. 4

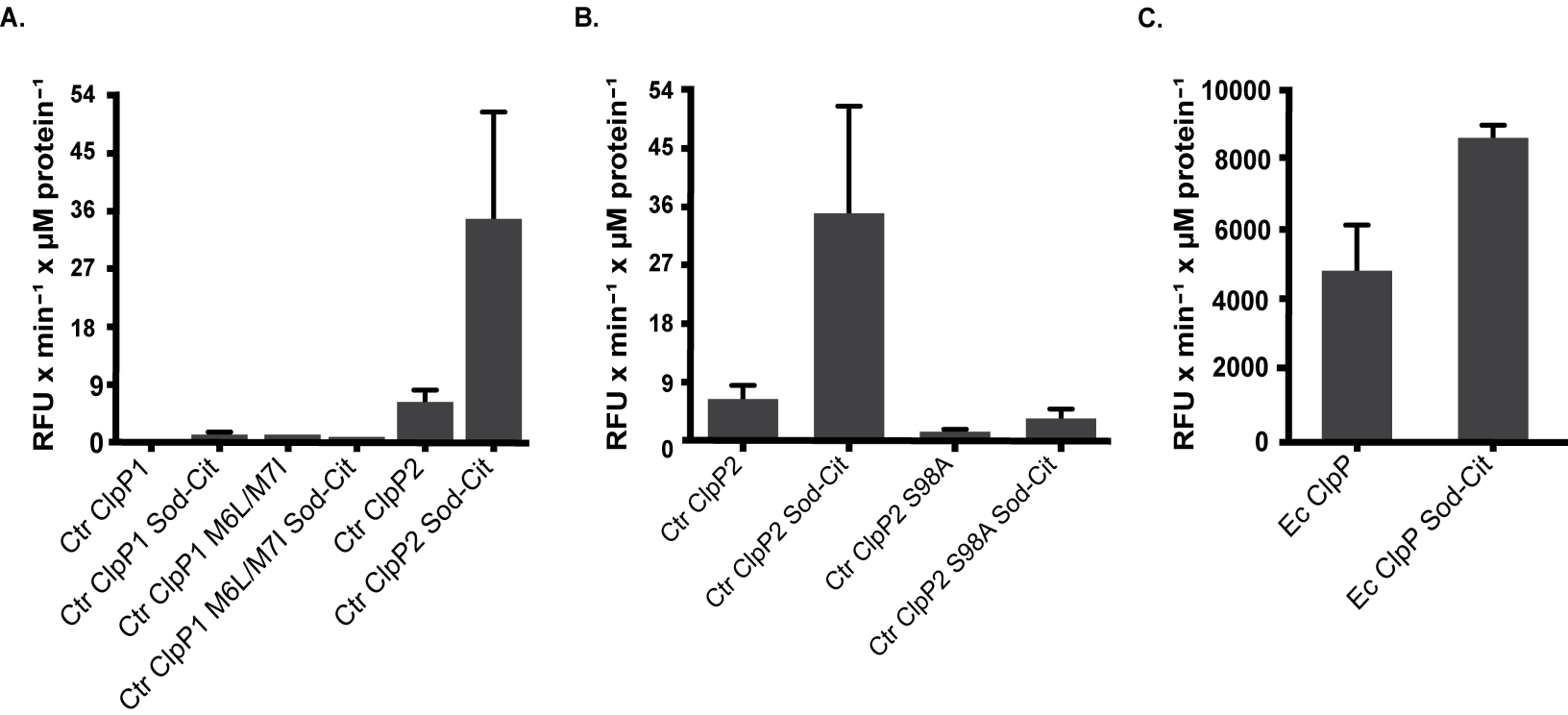
A.
RFU x min⁻¹ x µM protein⁻¹
54
45
36
27
18
9
0
Ctr ClpP1
Ctr ClpP1 Sod-Cit
Ctr ClpP1 M6L/M7I
Ctr ClpP1 M6L/M7I Sod-Cit
Ctr ClpP2
Ctr ClpP2 Sod-Cit
B.
RFU x min⁻¹ x µM protein⁻¹
54
45
36
27
18
9
0
Ctr ClpP2
Ctr ClpP2 Sod-Cit
Ctr ClpP2 S98A
Ctr ClpP2 S98A Sod-Cit
C.
RFU x min⁻¹ x µM protein⁻¹
10000
8000
6000
4000
2000
0
Ec ClpP
Ec ClpP Sod-Cit

Fig. 5

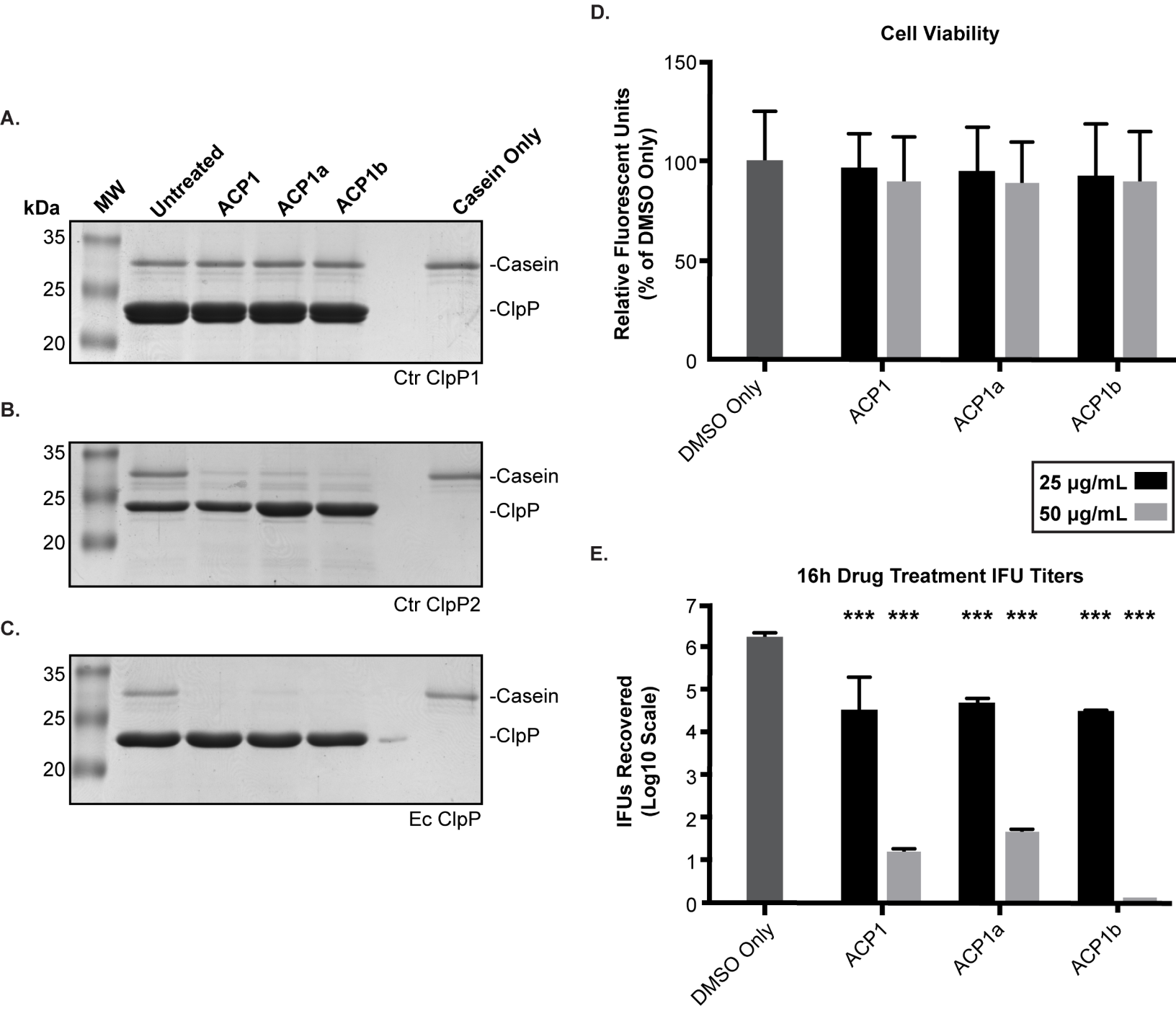
A.
kDa
MW
Untreated
ACP1
ACP1a
ACP1b
Casein Only
35
25
20
-Casein
-ClpP
Ctr ClpP1
B.
35
25
20
-Casein
-ClpP
Ctr ClpP2
C.
35
25
20
-Casein
-ClpP
Ec ClpP
D.
Cell Viability
Relative Fluorescent Units
(% of DMSO Only)
150
100
50
0
DMSO Only
ACP1
ACP1a
ACP1b
25 µg/mL
50 µg/mL
E.
16h Drug Treatment IFU Titers
IFUs Recovered
(Log10 Scale)
7
6
5
4
3
2
1
0
***
DMSO Only
ACP1
ACP1a
ACP1b

Fig. 6